

## Validation and Verification of Component Models and System Models for the PV Toolbox

Prepared by:  
Dr. Didier Thevenard & Michael Ross  
Numerical Logics Inc.  
6722 Dawson Street  
Vancouver, British Columbia  
V5S 2W3 Canada

Presented to:  
Dave Turcotte & Farah Sheriff  
CANMET Energy Diversification Research Laboratory  
Natural Resources Canada

Under contract #23332-9-0001/001-SQ

March 28, 2002

## Summary

The component models of the PV Toolbox have been validated and verified according to standard software engineering practices. The component models used for weather modelling required significant changes; other models required only minor corrections. These changes have been implemented. Thus the following component models can be considered valid and operational: weather modelling routines, PV generators, thermal mass, fuel reservoir, genset, and inverter.

The component models were assembled into system models ranging from a simple PV-load system to a full hybrid system. System model testing revealed that while the components functioned well in isolation, they caused the Simulink<sup>®</sup> simulation engine to freeze or halt due to difficulty in resolving the system of equations corresponding to the system model. Through various modifications to the component models, these difficulties were overcome. Subsequently, 12 system models were tested. Eleven of these were able to run for one simulation year without problem; the twelfth stopped only because the test parameters had permitted the battery to reach a low state-of-charge outside of the range of normal conditions.

## Contents

Summary .....	i
1) Introduction .....	1
2) Component Model Testing Methodology.....	1
3) Weather Modelling.....	2
3.1) Assumed Goal of Weather Modelling Routines .....	2
3.2) Examination of Weather Modelling Approach .....	2
3.2.1) Tilted Total Solar Irradiance/Radiation .....	2
3.2.1.1) Outline of Approach Used.....	3
3.2.1.2) Relevant Time-series Characteristics .....	4
3.2.1.3) Problem with Existing Approach: Unknown Serial Correlation.....	6
3.2.1.4) Problem with Existing Approach: Improper Probability Distribution .....	8
3.2.1.5) Problem with Existing Approach: Hourly Clearness Index is Fully Deterministic.....	8
3.2.1.6) Problem with Existing Approach: Profile of Irradiance Through Day is Incorrect .....	9
3.2.1.7) Concerns about Existing Approach: Input Parameters are Ambiguous ....	10
3.2.1.8) Concerns about Existing Approach: Correlation not Validated .....	11
3.2.1.9) Concerns about Existing Approach: Possible Improper Use of Correlation .....	11
3.2.1.10) Concerns about Existing Approach: Input to Albedo Calculation .....	11
3.2.1.11) Concerns about Existing Approach: Better Slope Irradiance Models Exist .....	11
3.2.2) Ambient Air Temperature.....	12
3.3) A Change in the Approach of the Weather Modelling Routines .....	14
3.3.1) Watgen Verification.....	15
3.4) Validation of the Revised Weather Modelling Routines .....	18
3.5) White Box Verification of the Weather Modelling Routines .....	19
3.6) Black Box Verification of the Weather Modelling Routines.....	21
3.7) Changes .....	22
3.8) Final Black Box Testing.....	24
4) Photovoltaic Generator Modelling .....	27
4.1) Photovoltaic Module Thermal Model .....	28
4.2) The Model for Photovoltaic Array at Maximum Power Point.....	28
4.3) The PV Module Model.....	33
4.4) Changes to the Models Following Validation.....	35
4.5) Verification of the Model for Photovoltaic Array at Maximum Power Point .....	35
4.6) Verification of the Model for the PV Array.....	36
5) Thermal Mass and Fuel Reservoir Model .....	38
5.1) Thermal Mass Model .....	39
5.2) Fuel Reservoir Thermal Model .....	39
5.3) Application of the Models.....	40
6) Inverter Model .....	42
6.1) Validation.....	42
6.2) Verification.....	49
7) Genset .....	49

7.1) Validation .....	49
7.2) Verification.....	51
8) Other components.....	51
9) System Models .....	52
9.1) Background .....	52
9.2) Approach and Procedure .....	53
9.3) System Model Tests .....	54
9.3.1) PV MPPT Array/Load .....	54
9.3.2) PV Array/Load.....	54
9.3.3) PV MPPT Array/Battery/Load .....	55
9.3.4) PV Array/Battery/Load.....	55
9.3.5) PV MPPT Array/Battery/Charge Controller/Loads.....	56
9.3.6) PV Array/Battery/Charge Controller/Loads .....	56
9.3.7) PV MPPT Array/Battery/On-Off Charge Controller/Loads .....	57
9.3.8) PV Array/Battery/On-Off Charge Controller/Loads .....	57
9.3.9) PV MPPT Array/Battery/On-Off Charge Controller/Loads/Inverter .....	58
9.3.10) Genset/Battery/Control Center/Loads/Inverter/Rectifier.....	58
9.3.11) PV MPPT Array/Genset/Battery/Control Center/Loads/Inverter/Rectifier...	60
9.3.12) PV Module/Genset/Battery/Control Center/Loads/Inverter/Rectifier .....	62
10) Conclusions .....	62
References.....	63

## 1) Introduction

The hybrid systems project at CEDRL will involve using simulation, backed up by real system performance data, to optimize the energy flows within a PV/battery/genset systems. The simulations will use a package of models implemented in the Matlab<sup>®</sup>/Simulink<sup>®</sup> environment. An attempt has been made to model all pertinent aspects of the power system (e.g., photovoltaic modules, genset, battery, etc.) and the environment (radiation and temperature, etc.).

This document reports on the methodology used to test these models and their implementation, and describes the shortcomings in the models that were identified during testing. Testing was conducted in two stages: component model testing (covered in Sections 3 through 7 of this report), which examined the behaviour of the PV Toolbox components in isolation, and system model testing (covered in Section 9), which ensured that the component models can be assembled into functioning system models.

## 2) Component Model Testing Methodology

The author, hereafter referred to as the “tester”, has used the following procedure to validate and verify the hybrid system modelling library. The procedure is grounded in standard software testing practices, e.g., as outlined in [IPL, 1996].

1. Statement of Goal: The first step in the procedure is to state the goal of a routine or ensemble of inter-related routines, as perceived by the tester<sup>1</sup>. This is necessary for several reasons:
  - In order to determine whether a routine works, one must have an idea of what it is supposed to do.
  - It establishes that the tester adequately understands the intentions of the creator of the routine.
  - It helps define the limits of validation.
2. Validation of Approach: Once the goal of a routine has been stated, the tester examines the theory behind the approach taken by the creator of the routine. The tester must determine whether the approach taken can be reasonably expected to satisfy the stated goals. Here the tester searches for fundamental flaws or theoretical inaccuracies in the approach.
3. “White box” verification: Having stated the goal of a routine and validated the theoretical approach used to attain this goal, the tester examines how the approach has been implemented, attempting to identify inaccuracies or errors in the model algorithms. In short, white box investigation entails a comparison between theory and implementation.
4. “Black box” verification: With approach validated and algorithms verified, the tester examines the input-output behaviour of the routine and, without reference to the workings of the model, verifies that this behaviour is reasonable.

---

<sup>1</sup> In the language of software development, this is similar to a “requirements specification”.

5. Identification of options and making of recommendations: When an error or inaccuracy is uncovered, the tester investigates the consequences of the error or inaccuracy, identifies the options for correcting the problem, and makes a recommendation. The obvious solution to simple errors uncovered during white box investigation may be a straightforward fix to the code. For inaccuracies in the approach, however, options and recommendations will hinge upon 1) whether the inaccuracy will materially impact the accuracy of the simulation as a whole, and 2) whether better approaches exist, and if so, whether they are sufficiently tractable.

While the procedure above has been presented as a sequence of steps to be carried out one after the other, in reality the tester may proceed with several steps at once, or return to a “prior” step to clarify findings. For example, an examination of approach may entail both a white box investigation when the creator’s approach is not clearly stated in the documentation and a black box investigation when the validity of the approach must be tested.

### **3) Weather Modelling**

For the purposes of testing, the weather modelling routines include all those in the “Weather” and “Accessories” blocks.

#### **3.1) Assumed Goal of Weather Modelling Routines**

Broadly stated, the goal of the weather modelling routines is:

For a given location, generate a time-series of weather data that would mimic measured data from that location such that conclusions based on simulation runs would not depend on whether measured or generated data was used.

The tester assumes that:

- Only two weather variables are significant to hybrid system modelling: the ambient air temperature and the average total solar irradiance (or total solar radiation) over the time step on an arbitrarily oriented, unshaded surface. These will be the outputs.
- The inputs to the routine will be monthly statistics characterizing the ambient temperature and global solar radiation (i.e., on the horizontal) for the given location, as well a specification of the location, the surface orientation, and the starting and ending times of the simulation.
- The time-step will be one hour at maximum.
- The time-series will not be limited in duration.

#### **3.2) Examination of Weather Modelling Approach**

##### **3.2.1) Tilted Total Solar Irradiance/Radiation**

### 3.2.1.1) Outline of Approach Used

The creation of an hourly time-series for the insolation in the plane of the array involves a rather complicated multi-step procedure. As a starting point for discussion, the procedure currently used is outlined below. Note that the inputs to the procedure are the mean daily insolation,  $H_{month}$ , for each month, and the standard deviation of the daily insolation for each month,  $\sigma_H$ , calculated by:

$$\sigma_H = \sqrt{\frac{1}{n} \sum_{month} (H - H_{month})^2}$$

where  $H$  is the daily total insolation on the horizontal and  $n$  is the number of days in the month. The procedure makes use of random numbers generated according to a “narrowed random” distribution. This is a normal distribution truncated at a high and low threshold, with the consequent effects on the variance and mean corrected by the addition of offsets to subsequent values for the random variable; this procedure and the distribution are discussed further below.

The procedure used is:

- i) Generate  $H_0$ , the extraterrestrial insolation on a horizontal surface for the day, using Eq. 1.10.3 from [Duffie et al., 1991].
- ii) Generate  $H$ , the total insolation on the horizontal for the day. This is generated using a “narrowed random” distribution with parameters
  - mean daily insolation for the month ( $H_{month}$ )
  - the standard deviation of the daily insolation over the month,  $\sigma_H$
  - a high threshold of  $0.88H_0$
  - a low threshold of  $0.04H_0$

Thus, this step is equivalent to generating a daily clearness index,  $K_T$ , that has a narrowed random distribution. The distribution has a mean of  $K_{T,month}$ , the monthly clearness index; its standard deviation is related to the standard deviation of the daily clearness index, and thresholds of 0.88 and 0.04.

- iii) Generate a sequence of the total insolation on the horizontal,  $I$ , for each hour during the day (represented by the continuous variable  $t$ , time in hours). The sequence is assumed to have the form of a half-sinusoid:

$$I(t) = \max \left[ 0, \frac{H\pi}{2D} \sin \left( \frac{\pi}{D} (t - T_R) \right) \right]$$

where  $T_R$  is the time of sunrise and  $D$  is the length of day. The sine function is multiplied by a term that equates the integral of  $I$  over the day and  $H$ .

- iv) Calculate a daily clearness index from  $H$ :

$$K_T = \frac{H}{H_0}$$

- v) Find a value for  $\sigma_I$ , the standard deviation of the hourly total insolation on a horizontal surface over the day. This is found from a correlation between the average hourly clearness index for a day and the standard deviation for the hourly

- clearness index. The correlation was developed by fitting a function to 1998 data from the weather station on the roof of the CEDRL.
- vi) Generate a value for  $k_T$ , the hourly clearness index, for each hour of the day. The hourly clearness index is generated as a random number with “narrowed random” distribution and parameters
    - mean of  $K_T$
    - standard deviation of  $\sigma_I$ , with the standard deviation limited to values greater than 0.05 for very clear days and 0.025 for very cloudy days.
    - a high threshold of 0.95
    - a low threshold of 0.01
  - vii) Find a value of  $\alpha$ , the ratio of diffuse insolation to total insolation on the horizontal. This is found using a correlation between  $k_T$  and  $\alpha$  given as Eq. 2.10.1 in [Duffie et al., 1991].
  - viii) Calculate  $I_d$ , the diffuse radiation on the horizontal:
 
$$I_d = \alpha I$$
  - ix) Calculate the beam radiation on the horizontal,  $I_B$ , from
 
$$I_B = I - I_d$$
  - x) The diffuse radiation in the plane of the array,  $I_{d,tilt}$ , is calculated from  $I_d$  using an isotropic sky model.
  - xi) The beam radiation in the plane of the array,  $I_{B,tilt}$ , is calculated by multiplying  $I_B$  by  $R_B$ , the ratio of tilted to horizontal beam radiation. The factor  $R_B$  is calculated using Eq. 1.8.1 from [Duffie et al., 1991].
  - xii) The albedo,  $\rho_g$ , is calculated by linear interpolation between a minimum and maximum albedo of 0.2 and 0.7 on the basis of temperature: at  $-5^\circ\text{C}$  and temperatures below, the albedo is 0.7; at  $0^\circ\text{C}$  and temperatures above, the albedo is 0.2.
  - xiii) The reflected radiation in the plane of the array,  $I_{r,tilt}$ , is calculated by multiplying  $I$  by the view factor of the ground and the albedo.
  - xiv) Total radiation in the plane of the array is the sum of the diffuse, beam, and reflected radiation in the plane of the array.

### 3.2.1.2) Relevant Time-series Characteristics

In order for synthesized weather data to mimic measured weather data, the two time-series must be alike in terms of:

- 1) Probability density function.
- 2) Serial correlation.

Measured weather data can be considered the product of the extraterrestrial radiation and a clearness index (ignoring that radiation which occurs before sunrise and after sunset). The extraterrestrial radiation is fully determined by the spatial relationships between the sun and the earth. The clearness index, on the other hand, is a stochastic variable.

The probability density function of the daily clearness index has been the subject of several investigations. These have concluded that the density function appears as shown in Figures 3.1 and 3.2 below. The cumulative distribution curves have been found to be

“very nearly identical for locations that have the same values of  $K_{Tmonth}$ , even though the locations varied widely in latitude and elevation” [Duffie et al., 1991, p. 78]. The hourly clearness index is similarly distributed.

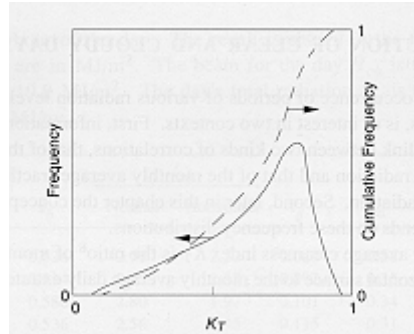


Figure 3.1. Probability Density Function and Cumulative Distribution Function for the Daily Clearness Index ([Duffie et al., 1991])

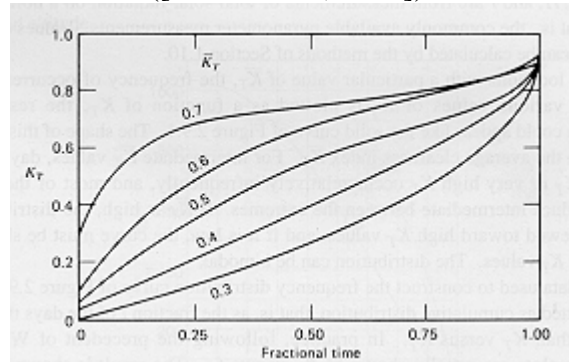


Figure 3.2. Typical Cumulative Distribution Functions for the Daily Clearness Index as a Function of the Monthly Clearness Index ([Duffie et al., 1991])

It is evident that the clearness index is not normally distributed; thus the daily or hourly insolation should not be normally distributed. This is confirmed in [McKay et al., 1985]: “The population of daily (or hourly) solar radiation values is in general not normally distributed.”

The probability density function for the clearness index (or the insolation) would fully characterize that variable were its time-series a sequence of independent random variables. It is not, however: the clearness index has a strong temporal trend, observable on time-scales of days and shorter, originating in the time required for weather systems to move over a given location and change the clearness index. Thus, if it is very cloudy one hour, it is likely to be cloudy the next, and if it is sunny one day, there is a good chance, even in maritime climates, for it to be sunny the next [Brinkworth, 1977]. This has long been recognized in the study of radiation time-series (for example, see the publications referenced in [Mora-López et al., 1998] and [Graham et al., 1990]).

Both the probability density function and the serial correlation of the radiation time-series will strongly influence the simulated behavior of a PV-hybrid system when an hourly or daily time-step is used; of the two, it is likely that the serial correlation is the more critical parameter, however. The probability density function is important insofar as the system being modelled is nonlinear. A system whose input-output relations were fully

linear could be simulated for the most part using just the mean value and some statistic of the variance of the radiation; the power output of the photovoltaic array is, as a first approximation, linearly related to the irradiance it sees. On the other hand, PV hybrid systems exhibit memory, due to battery storage, that extends over a period of up to days or weeks. Simulations based on radiation time-series which are unrepresentative in terms of serial correlation will likely be inaccurate. For example, consider a site where the radiation is strongly serially correlated: the probability of a three day run of cloudy weather would be high. For a PV-hybrid system having two days of autonomy, a simulation based on a radiation time series with strong serial correlation would show more frequent genset starts than a simulation based on each day's insolation being considered an independent random event.

### 3.2.1.3) Problem with Existing Approach: Unknown Serial Correlation

In the existing approach to weather generation, the hourly time series is serially correlated. This serial correlation arises indirectly in two ways: through the narrowed random number generation procedure and through the correlation used to relate the standard deviation of the hourly clearness index with the clearness index for the day.

The procedure to generate narrowed random numbers involves three steps. First, a normally distributed random number with specified mean and variance is generated. Second, the random number is compared with a specified upper and lower threshold: if the random number exceeds one of these thresholds, it is set to the threshold exceeded. Third, subsequent values of the random number are adjusted to correct for the reduction in the variance and the shifting of the mean caused by setting the out-of-range value to the threshold.

Unlike a normal random number sequence, in which the values are independent, the output of the narrowed random number generating sequence can be serially correlated. Whenever a number falls out of the thresholds, the narrowed random number algorithm adjusts subsequent values to correct for the changes to mean and variance caused by setting the out-of-bounds value to the threshold. Thus, the probability density function for a value is conditioned on whether the previous value is equal to one of the thresholds. Put another way, one's chances of guessing the output of the algorithm improves if one knows that the previous value was equal to one of the thresholds.

The narrowed random number generation procedure is used in two places: for the insolation for the day, in step ii above, and for the hourly clearness index, in step vi. Both of these variables exhibit serial correlation in reality. Thus the question is whether the narrowed random number procedure gives rise to a realistic form of serial correlation.

Because the serial correlation is imparted to the time-series indirectly rather than through some standard stochastic method, it is difficult to fully evaluate the serial correlation that the procedure will give rise to without generating a sequence of values and determining the autocorrelation coefficients. Intuitively, it seems unlikely that this algorithm would happen to automatically generate appropriately serially correlated sequences. Furthermore, it is possible to identify several characteristics of the procedure's output that are unrealistic:

- 1) Serial correlation arises from this procedure only when a value falls outside the upper or lower thresholds. For generating the daily insolation, these thresholds are set to 0.88 and 0.04 times the extraterrestrial daily insolation on the horizontal, respectively. When the mean daily terrestrial insolation on the horizontal is well within these limits, and its standard deviation is relatively small, it is unlikely that the thresholds will be exceeded. Thus, serial correlation will not occur, and the daily insolation sequence for the month will consist of serially uncorrelated (i.e., independent) random events. This is unrealistic.

For example, for Montréal in the month of July, the mean daily insolation on the horizontal is  $20.794 \text{ MJ/m}^2$  and its standard deviation is  $6.2392 \text{ MJ/m}^2$ . The lower and upper thresholds will be approximately 0.04 times  $40.5 \text{ MJ/m}^2 = 1.62 \text{ MJ/m}^2$  and 0.88 times  $40.5 \text{ MJ/m}^2 = 35.6 \text{ MJ/m}^2$ . These thresholds are 3.07 and 2.37 standard deviations away from the mean, respectively. The probability that a normally distributed random number will fall outside these limits is 1%. Thus only about one out of every three months of July data for Montréal will show any sign of serial correlation.

- 2) Other researchers have concluded that the daily radiation data series can be adequately described by a first-order Markov process [Lorenzo et al., 2000], [Brinkworth, 1977] (though the series is not stationary [Graham et al., 1990]) and the use of first-order autoregressive models is standard [Graham et al., 1988]. With the narrowed random procedure, serial correlation is not limited to first order correlations (i.e., between one value and the very next). For example, if a value exceeds a threshold, subsequent values will be modified and thus become correlated. But the modification will not necessarily appear in the very next value: if correcting the next value would, for example, correct the variance but move the mean in the wrong direction, the adjustment will not be effected until a later value, and serial correlation will be higher than first-order.
- 3) The narrowed random algorithm will lead to serial correlation of extreme values (i.e., threshold values) only. When values lie within the thresholds, no serial correlation occurs. When an out-of-bounds value is encountered, subsequent values are serially correlated—they will also have a tendency to be set to that threshold. This is equivalent to saying that only when today's weather is perfectly clear or fully overcast does it give any intimation of tomorrow's weather. This is not realistic, and other attempts to generate artificial radiation sequences have assumed that first-order serial correlation applies to all clearness conditions, not just extremes.
- 4) The narrowed random algorithm will likely lead to an element of negative serial correlation. Setting an out-of-bound value to a threshold requires a correction for the mean and the variance. The correction required for the mean will be linearly related to the difference between the out-of-bounds value and the threshold; the correction for the variance will be related to the square of the difference between the out-of-bounds value and the mean. Correcting for the variance will therefore tend to overcompensate for the shift in the mean. This will require that a subsequent value be adjusted in the opposite direction. This suggests that there may be a second or higher order negative serial correlation.

There may be other problems with the serial correlation that the narrowed random algorithm gives rise to; it is difficult to predict the characteristics of the algorithm's output. It does appear certain, however, that under some conditions, described above, its output will be unsatisfactory or unrepresentative.

The above discussion has dealt principally with serial correlation in the daily clearness index. Similar considerations apply to the hourly clearness index. Additional concerns about the serial correlation in the hourly clearness index are raised below.

#### 3.2.1.4) Problem with Existing Approach: Improper Probability Distribution

Section 3.1.2.2 described the observed probability density function for the daily and hourly clearness index and pointed out that the daily and hourly insolation are not normally distributed. With the current approach to generating insolation time-series, the daily insolation will be distributed according to the "narrowed random". How does this compare with the known probability density function?

When no value falls out-of-bounds, the output of the narrowed random algorithm will be normally distributed. As pointed out above, this is not a realistic distribution for the clearness index or the daily insolation. It is difficult to estimate to what extent this will detrimentally affect a simulation, however, without actually running simulations using both distributions.

When a value falls out-of-bounds, the distribution will deviate from the normal distribution in two ways:

- 1) The probability density function will be zero outside of the thresholds (as desired) but "spikes" will form at the thresholds, as if an impulse function, shifted to the threshold and scaled by the integral of the probability density function over the range beyond the threshold, were superimposed on the probability density function. This is clearly unrealistic.
- 2) The distribution will probably flatten and perhaps a peak will develop between the mean and the threshold nearest to the mean. The extent to which this will occur will depend on the extent to which the correction of mean and variance leads to values set to the thresholds. If most corrections do not end in the thresholds, the flattening could result in a distribution similar to that described in Section 3.2.1.2. (but with spikes at the thresholds).

Thus, the probability density function will be unrealistic to the extent that it is normal (all values within the thresholds) and to the extent that spikes appear in the probability density function at the thresholds. The flattening and shifting of the peak of the probability density function may be realistic, but this will not occur without the formation of unrealistic spikes.

#### 3.2.1.5) Problem with Existing Approach: Hourly Clearness Index is Fully Deterministic

Although an hourly clearness index is generated by a stochastic process in step vi of the existing approach, the hourly total insolation will appear to be fully deterministic. The generated "hourly clearness index" is never directly applied: it is used only as input to the relation that determines the fraction of the total radiation on the horizontal that is diffuse.

The hourly clearness index that will be apparent from the time-series arises in steps ii and iii, not step iv. In the first step, the narrowed random algorithm is used to generate a value for the daily insolation; this is nearly equivalent to generating a daily clearness index. In the second step, the hourly irradiance profile is generated as a half-sine wave which, when integrated over the day, is equal to the daily insolation. Thus the hourly clearness index is, as a first approximation, equal to the daily clearness index. Differences arise to the extent that the half sine wave does not represent the profile of irradiance on an extraterrestrial horizontal surface (discussed in the next section).

This is a problem for two reasons. First, the random variation in the horizontal irradiance over the course of the day is not modelled. The variation over the day always takes the form of a sine wave. Second, because the diffuse fraction is correlated to a “fake” hourly clearness index that is only loosely related to the apparent hourly clearness index, the ratio of beam to diffuse radiation will often be very unrealistic. This may have serious implications in terms of the hourly insolation in the plane-of-the-array: this will seem to contain a spurious random component.

### 3.2.1.6) Problem with Existing Approach: Profile of Irradiance Through Day is Incorrect

In step iii of the existing approach, a half-sine is used to model the variation in the irradiance over the course of the day. As mentioned above, this ignores the stochastic nature of the hourly insolation. Putting this criticism aside, there are two errors in this approach: it does not accurately model the extraterrestrial profile of irradiance on the horizontal, and it does not accurately model the deterministic effects of atmosphere on the terrestrial irradiance.

Variation in the extraterrestrial radiation on the horizontal, ignoring variation in the earth-sun distance and the solar “constant”, is due to the changing angle between the normal to the surface and the sun’s rays, i.e., the zenith angle. When this angle is zero, the extraterrestrial radiation on the horizontal is at a maximum; when the angle is 90° or greater, the radiation is zero. The existing approach accounts for this trend with a half-sine wave, indexed to the time of the day vis-à-vis sunrise and sunset.

In reality, the profile of irradiance on the extraterrestrial horizontal surface will have the form [Duffie et al., 1991, p. 16]:

$$\cos \theta_z = \cos \phi \cos \delta \cos \omega + \sin \phi \sin \delta$$

or

$$\cos \theta_z = \alpha \cos \omega + \beta$$

where  $\theta_z$  is the zenith angle,

$\phi$  is the latitude,

$\delta$  is the declination,

$\omega$  is the hour angle,

and  $\alpha$  and  $\beta$  can be considered constants for a given day. This is in contrast to the form used in the existing approach:

$$\cos \theta_z = \alpha \cos t$$

where  $t$  is a measure of time over the day.

The accurate approach will lead to a “flattening” of the irradiance profile at the beginning and end of the day whenever the location is not on the equator or it is not the equinox.

A second inaccuracy of the existing approach is that it ignores deterministic trends in the terrestrial irradiance profile. As the zenith angle increases, the amount of atmosphere through which the sun’s rays must pass increases. This will have an effect on the clearness index. Furthermore, as the sun approaches the horizon, reflections within the atmosphere become significant. This permits diffuse light to reach a horizontal surface even after the sun has set, especially at high latitudes.

These are relatively minor criticisms of the existing approach. Nevertheless, the first of the two is addressed relatively easily, and will lead to more realistic irradiance profiles over the day.

### 3.2.1.7) Concerns about Existing Approach: Input Parameters are Ambiguous

The input to the procedure for generating daily and hourly insolation time series includes the mean irradiance and the “standard deviation of irradiance”. While the mean irradiance is a fairly straightforward characteristic of the radiation at a site, the “standard deviation of irradiance” needs to be more clearly defined.

First, it must be noted that the irradiance is a continuous variable equal to the rate at which radiant energy is incident on a surface per unit of surface area. The standard deviation of this variable is not commonly available from measured weather data. Here we will assume that the input of interest is the standard deviation in the daily insolation for a given month.

Second, it must be further noted that the standard deviation of the daily radiation is defined in different ways in different sources. For example, in the Environment Canada *Canadian Climate Normals (Volume 1) Solar Radiation 1951-1980*, [Atmospheric Environment Service, 1982], the average daily insolation for the month is calculated for each year, and then the standard deviation is calculated using these averages. Thus, in this case the standard deviation is a measure of the year-to-year variability of the average daily insolation for a given month. In contrast, in the series *Solar Radiation Analyses for Canada 1967-1976* ([McKay et al., 1985]), the standard deviation seems to be calculated from the entire population of daily insolation values for a given month. With ten years of data, the population is around 300 values. Thus, in this case the standard deviation appears to be a measure of both the day-to-day variability and the year-to-year variability of the daily insolation for a given month.

It is not clear that any measure of the variability that includes the year-to-year variability is appropriate for an algorithm that generates a time series for a single year. At minimum, the part of the variability that is due to the year-to-year variability should be explicitly known. Great care should be exercised when taking this statistic from the literature, to ensure that it reflects only the day-to-day variability.

A third concern with this approach is the paucity of standard deviation data. World-wide, the mean daily insolation (or by extension, the mean daily clearness index) is readily available. The standard deviation, while available from Environment Canada, may not be available for many other locations.

### 3.2.1.8) Concerns about Existing Approach: Correlation not Validated

In step v of the existing approach, a correlation between the standard deviation of the hourly clearness index for a day and the average hourly clearness index for the same day is used as input to the procedure for generating the hourly clearness index. This correlation, based on a curve fit to one year's measured data from the meteorological station on the roof of the CEDRL, has not been validated. It is unknown whether it is applicable to other years' data for the same location, or data from other locations. In its favour, in a qualitative assessment it has the tendency one would expect from such a correlation. On the other hand, with a coefficient of determination ( $r^2$  value) of 0.46, the relation does not account for much of the variation in the data.

### 3.2.1.9) Concerns about Existing Approach: Possible Improper Use of Correlation

The correlation used in step v has, as independent variable, the “mean of  $k_T$ ”, the hourly clearness index for the day. It appears that when the correlation was determined the independent variable was calculated from:

$$k_T^* = \frac{1}{n} \sum_{day} k_T$$

where  $k_T^*$  is the mean of the hourly clearness index over the day,

$k_T$  is the clearness index for an hour during the day,

and  $n$  is the number of hours during the day during which there was light.

When this correlation is used in step v, however, the dependent variable is the daily clearness index. It should be noted that the daily clearness index is not equivalent to the mean of the hourly clearness index over the day. The latter variable weights the clearness index for each hour equally, while the daily clearness index in effect weights the clearness index for each hour by the extraterrestrial radiation during that hour.

It is unknown to what extent this difference will affect the time-series.

### 3.2.1.10) Concerns about Existing Approach: Input to Albedo Calculation

In step xii of the existing approach, the albedo is calculated as a function of temperature. It should be clarified that this temperature should be the monthly average temperature. The use of daily or hourly temperature may introduce unrealistic “high” frequency fluctuations in the albedo. It should be further noted that this relation is an adhoc measure that is used where no additional data is available.

### 3.2.1.11) Concerns about Existing Approach: Better Slope Irradiance Models Exist

In step x of the existing approach, the diffuse radiation on a tilted surface is calculated from the diffuse radiation on the horizontal surface assuming an isotropic sky. The isotropic sky, while the simplest of the sky models, is known to underestimate the diffuse radiation falling on a tilted surface with a component facing the south [Duffie et al., 1991, p.96], [Vartiainen, 2000]. It therefore represents not merely a random inaccuracy that could be hoped to disappear in average behaviour, but a bias “against”

photovoltaics. More accurate slope irradiance models exist; these are relatively straightforward to implement.

### 3.2.2) Ambient Air Temperature

The ambient air temperature is approximated by one period of a sinusoid, with its highest value two hours after noon and its lowest value two hours after midnight. The amplitude of the sine is the difference between the average measured maximum daily temperature for the month and the average measured minimum daily temperature for the month. The mean value of the sine corresponds to the average measured value for daily temperature for the month.

The temperature profile over the day is the same for all days in the month. Thus the temperature profile can be interpreted as the mean trend for temperature; stochastic variations have been ignored. This raises three questions:

- 1) Will ignoring stochastic variation in the temperature profile induce detectable error in the simulation?
- 2) Is the correlation between ambient temperature and irradiance modelled sufficiently accurately?
- 3) Is the sine wave approximation of the trend accurate?

The output of the PV modules can be considered, as a first approximation, to vary linearly with temperature. Thus, under normal circumstances the total output of the modules over a given period of time can be predicted using mean trend or average temperature data. There is one caveat, however: if temperatures are sufficiently high that the array voltage drops below the battery voltage (and no DC-DC converter such as a maximum power point tracker is used) then the output of the array is not utilisable. In general, however, modules will be selected to avoid this problem, and hybrid system simulations will not investigate these types of effects. Thus, ignoring stochastic variation in the ambient temperature will not significantly affect total array output.

A number of important battery performance characteristics are non-linearly related to temperature. These include corrosion and self-discharge reactions, the resistivity of the electrolyte, the discharge capacity, the gassing voltage, and the battery efficiency. As a first approximation, these characteristics (excepting corrosion and self-discharge reactions) can be considered to change linearly at temperatures down to roughly 0 or  $-5^{\circ}\text{C}$ ; indeed, they have been treated this way in the existing battery model. Thus, as long as the battery temperature does not fall below, say,  $-5^{\circ}\text{C}$ , ignoring stochastic variation in ambient temperature will not significantly affect battery performance. The corrosion and self-discharge reactions may tend to be underestimated, however, since accelerated rates at higher temperatures will not be accounted for. On the other hand, the battery model accounts for self-discharge and corrosion in a very approximate way, so it is not clear that ignoring stochastic variation in temperature will be a real limit on accuracy. Furthermore, the variation in temperature of the battery will be smoothed by any insulation around the battery and the thermal mass of the battery itself. This will reduce the inaccuracies associated with ignoring the stochastic variation in temperature.

In one respect, batteries behave highly non-linearly: certain combinations of current, temperature, and state-of-charge lead to very high overpotentials. That is, the battery can “run out of energy”. This is not merely an issue of linearity. Rather, the role of “memory” is significant. Lower battery temperatures reduce useable battery capacity and may therefore result in the battery failing to power the load. In stand-alone PV systems, this is a very significant event. In a hybrid system, the genset prevents this from occurring, and the event is far less significant. Thus, ignoring stochastic variation in temperature will lead to suspect results at cold temperatures with PV-only systems, but should be acceptable, as far as the battery is concerned, in hybrid systems.

The genset wear occurring during starting increases as temperature drops; it is not clear whether the relationship is linear over the temperature range of interest (at the very low temperatures at which lubricants solidify there is good reason to believe that it will be non-linear). It is difficult to start gensets at low temperatures; therefore it can probably be assumed that in the interest of system reliability some measure will be in place to regulate the genset temperature, such as insulation, thermal mass, etc. This will serve to limit the inaccuracies introduced by ignoring the stochastic variation in the ambient air temperature.

In summary, it should be acceptable to ignore the stochastic variation in ambient air temperature as long as the system being modelled:

- 1) Has measures in place to dampen swings in the battery temperature and to regulate the genset temperature, such that the temperature of these components does not fall to much below 0°C;
- 2) Or if the battery temperature will fall to much below 0°C, there is a genset or other device to provide power on demand;
- 3) Will not operate with the batteries at high temperatures for extended periods of time;
- 4) And is designed such that there is very low probability of high temperatures forcing the array voltage below the battery voltage.

Irradiance and ambient air temperature are correlated. Much of this correlation is implicit in the models and the input data. For example, higher average monthly temperatures during the summer months reflect, in part, higher insolation during this season. The sinusoid used to model temperature variation over the day accounts for solar heat gains during the day and radiation losses at night. Intuitively, it seems that the model used accounts for the correlation between the average daily irradiance profile for the month and the average daily temperature profile for the month. But considerable stochastic variation is superimposed on the average daily irradiance profile. It is clear that since there is no stochastic component to the temperature profile, any non-zero correlation between the stochastic variation in irradiance and the variation in temperature is not accounted for.

It appears that the main way in which this correlation will affect the system is through the battery. If particularly cold periods, which reduce battery useable capacity, are strongly correlated with sunshine levels then ignoring the correlation will lead to incorrect conclusions about 1) the loss-of-load probability in a PV/battery system and 2) genset cold starts in hybrid systems. The tester speculates, however, that the correlation between temperature and insolation is less important than either of these factors

considered individually. Furthermore, the accuracy of the current battery model declines significantly at temperatures below  $-5^{\circ}\text{C}$ , implying that in cold climates there will be some mechanism to regulate battery temperature. This or any other mechanism (insulation, thermal mass, etc.) that dampens the swings in battery temperature will help to decouple variation in temperature and insolation. Ignoring the correlation between stochastic variations in irradiance and temperature should not, therefore, limit the simulation accuracy, especially for hybrid systems.

The last question to be answered is whether the sinusoidal approximation of the temperature profile is an accurate representation of the average daily trend in temperature. Other synthetic weather generators (e.g., Meteonorm [Remund, 1997]) use smoothed irradiance data to generate the trend for temperature. Since the trend for irradiance roughly follows a sinusoid over the day, the daytime temperature trend seems reasonable. The two hour lag used in the current method is comparable to the 2 or 3 hour lag used elsewhere [Remund, 1997]. Other synthetic weather generators typically extrapolate the daytime trend until sunrise [Remund, 1997]. In the current method, temperature starts to rise at 2 AM. This may be physically inaccurate, but PV system simulation should not be affected by whether the minimum temperature occurs at 2 AM or some other time in the early morning. The current method will tend to underestimate the gradient of temperature rise through the morning whenever sunrise occurs after 2 AM.

The only major concern with the current method arises when the average daily maximum and average daily minimum temperatures are not equally far from the average daily temperature: the average daily maximum and minimum temperatures generated by the method will not match the model input. This occurs because the difference between the maximum and the minimum determines the amplitude of the sinusoid, but the sinusoid is centered on the average daily temperature.

It seems likely, however, that all inaccuracies in the use of a sinusoid to represent the daily trend for temperature are dwarfed by those caused by ignoring stochastic variation in temperature. Since we have already accepted those inaccuracies, the sinusoid seems acceptable.

Though the current method is acceptable, a preferable method may be that of Erbs, Klein, and Beckman [Erbs et al., 1983]. This method is based on measured data from nine sites in the US and therefore may be more accurate than an ad hoc method. It has the additional advantage of requiring only the monthly clearness index and the monthly average temperature as input.

### **3.3) A Change in the Approach of the Weather Modelling Routines**

Following the above validation, extensive changes were made to the weather modelling routines. The existing approach of synthesizing weather data within the Simulink<sup>®</sup> model was replaced by a two step approach:

- 1) Watgen, an existing synthetic weather generator, is used to generate a “TMY” file for the location.
- 2) The TMY file output of Watgen is read by the Simulink<sup>®</sup> toolbox during model initialization.

Thus the weather modelling routines no longer perform radiation or temperature synthesis; this is left up to Watgen. On the other hand, the weather modelling routines still include the code required to estimate the radiation in the plane of the array given hourly global insolation data on the horizontal.

These changes required further validation. First, the output of the Watgen synthetic weather generator was investigated. Second, the revised routines in the weather modelling toolbox were validated and verified. As part of this process, some important changes were made to the routines. The tester implemented these changes directly. As a final check, the tester compared the output of the routine with that of Watsun PV for several locations.

### 3.3.1) Watgen Verification

When CEDRL started work on the weather modelling routines they considered the possibility of using Watgen. This approach was not pursued, however, because a test of the program using Environment Canada monthly means suggested that the variance of the Watgen output was significantly different from the measured variance. Before relying on Watgen to generate data for the hybrid systems toolbox, therefore, the tester had to establish whether the output of Watgen was, in fact, realistic.

In order to do this, the monthly mean and standard deviation of Watgen-generated daily global radiation on the horizontal was compared with measured statistics. Four sources of measured data were used:

- 1) Hourly data measured on the rooftop of CEDRL for the year of 1998.
- 2) Hourly data measured at the Iqaluit Arctic College in the year of 2000.
- 3) Monthly mean and standard deviation for daily insolation for St. Hubert, Quebec, as tabulated in Solar Radiation Analyses 1967 to 1976 from Environment Canada [McKay et al., 1985].
- 4) Monthly mean and standard deviation for daily insolation for Montreal as tabulated in the Canadian Climate Normals of Environment Canada for 1951 to 1980 [Atmospheric Environment Service, 1982].

The hourly data from CEDRL and the Iqaluit Arctic College were cleaned up (i.e., night-time values set to zero, missing or suspect data sections removed, etc.) Then the monthly values for the mean, standard deviation, skew, and kurtosis of the daily insolation were determined. The means from CEDRL, Iqaluit, and Environment Canada were used as input to Watgen; the output was analysed for monthly mean, standard deviation, skew and kurtosis. Finally the mean and standard deviation values (both measured and generated by Watgen) were plotted as a time-series for comparison purposes.

The “TMY” option in Watgen was normally selected. This constrained the output of Watgen such that the mean output value for each month closely matched the input mean for the month. For the Iqaluit and Varennes data, Watgen was also tested using the “Any” year option, which removed this constraint. Various seeds were tried. The output is plotted in Figures 3.3 through 3.7.

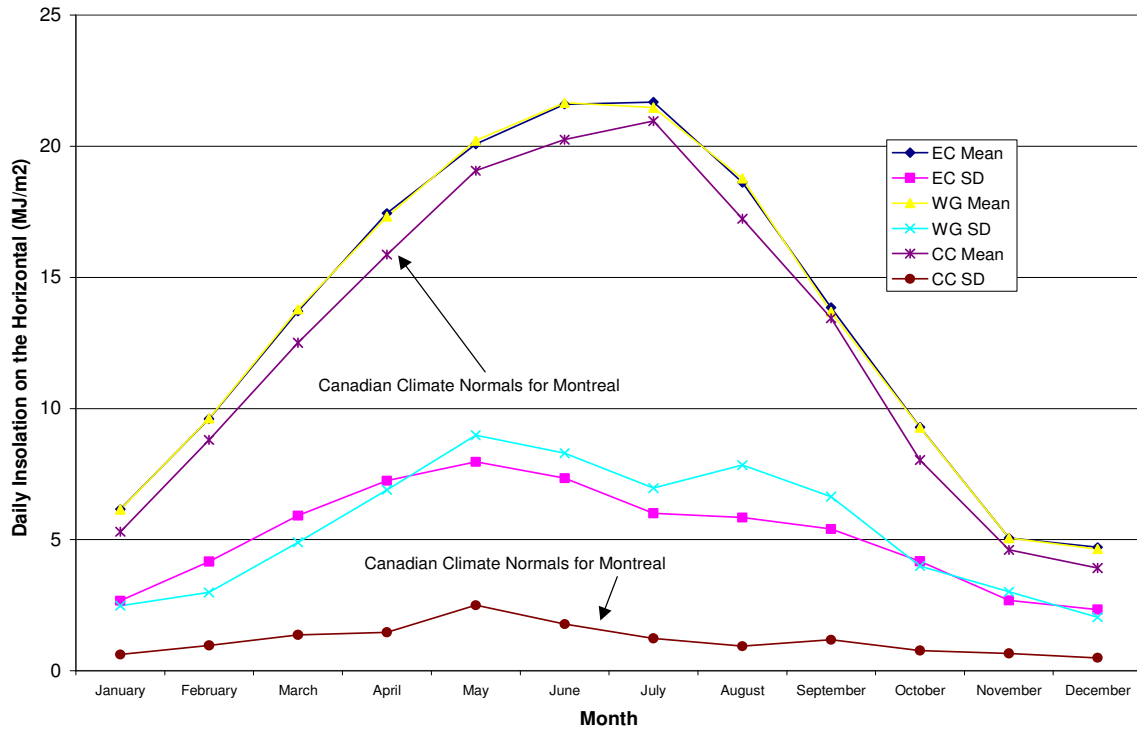


Figure 3.3 Mean and Standard Deviation for Daily Insolation at St. Hubert: Environment Canada Solar Radiation Analyses and Climate Normals versus Synthesized

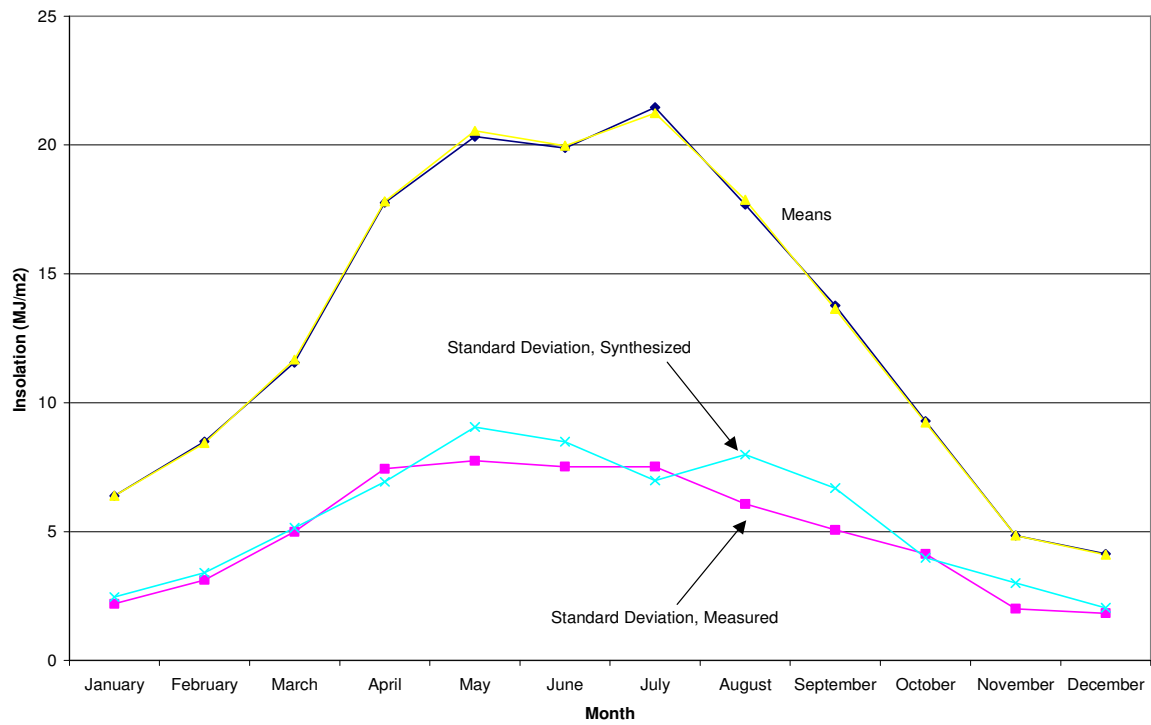


Figure 3.4 Mean and Standard Deviation for Daily Insolation at Varennes, 1998: Measured versus Synthesized

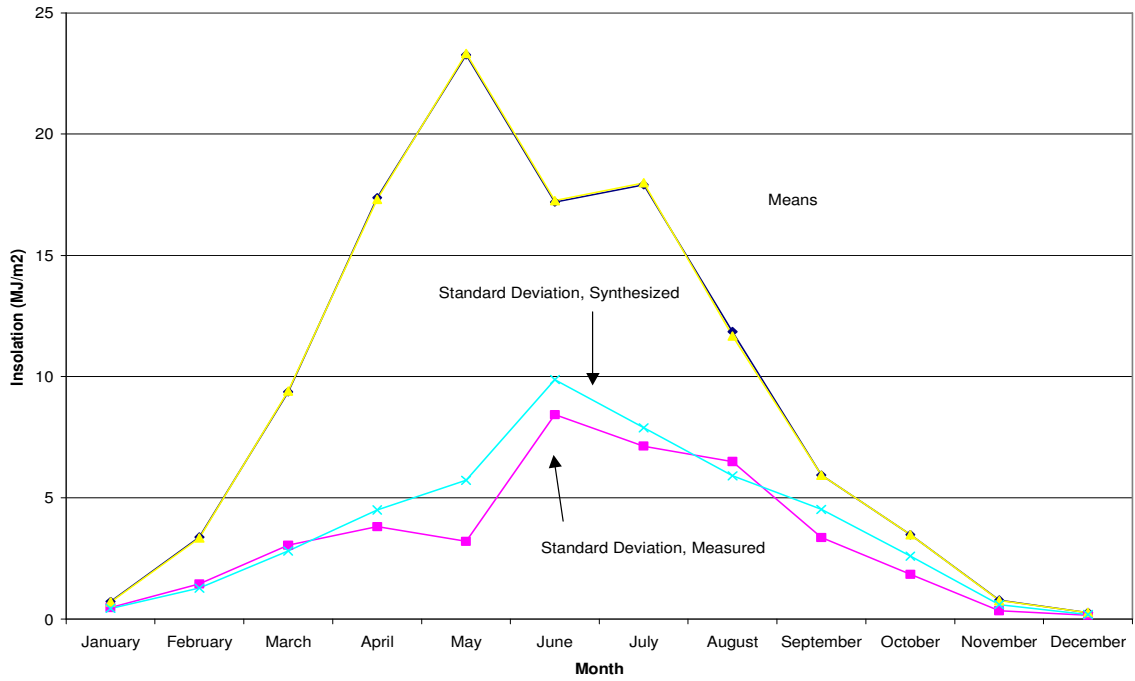


Figure 3.5 Mean and Standard Deviation for Daily Insolation at Iqaluit, 2000: Measured versus Synthesized

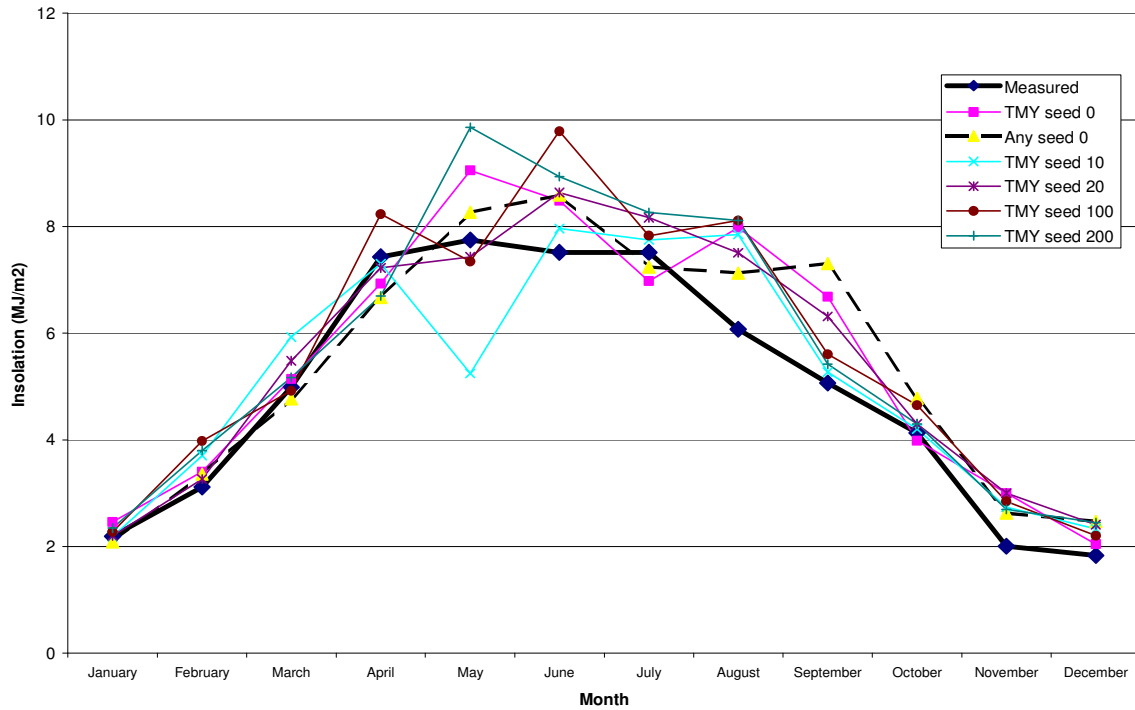


Figure 3.6 Standard Deviation for Daily Insolation at Varennes, 1998: Measured versus Synthesized

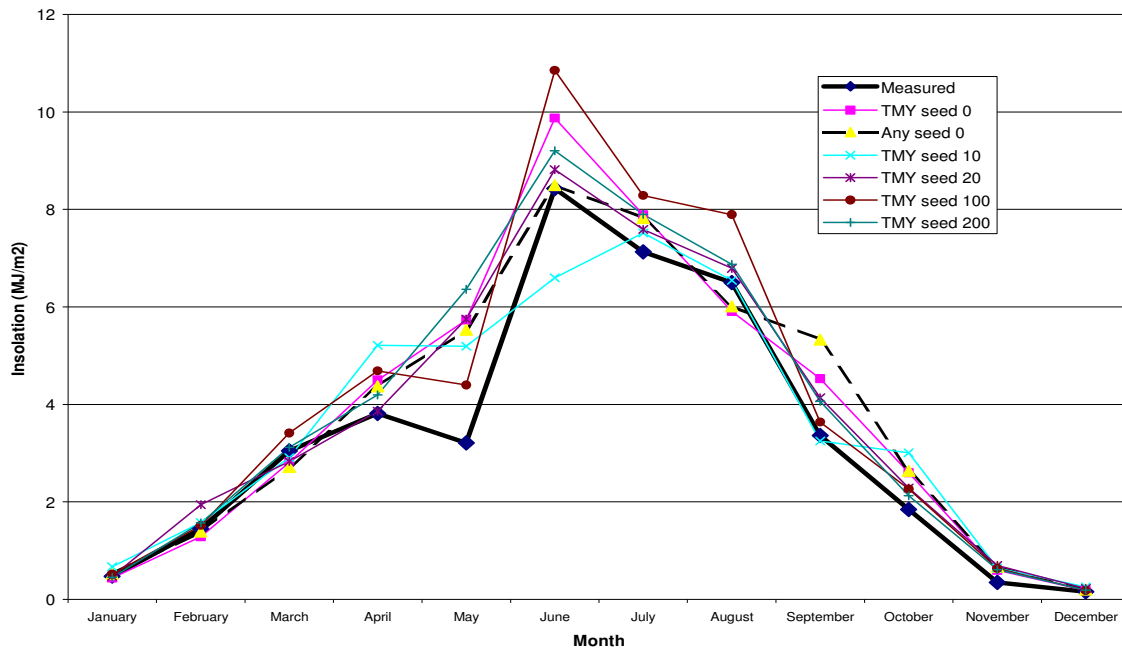


Figure 3.7 Standard Deviation for Daily Insolation at Iqaluit, 2000: Measured versus Synthesized

CEDRL and the tester concluded from the figures above that the standard deviation of daily insolation for Watgen output was sufficiently close to the measured standard deviation that Watgen could not be dismissed on this basis. The tester hypothesized that the original test, from which it was concluded that Watgen did not recreate the variance in measured data, had used Canadian Climate Normals. The standard deviation in the Canadian Climate Normals is a measure of the inter-year variability, however, and is not comparable with the standard deviation of daily insolation, as shown in Figure 3.3.

Following the investigation described above, CEDRL concluded that Watgen could be used for synthetic weather generation for its hybrid system modelling toolbox.

### 3.4) Validation of the Revised Weather Modelling Routines

Having eliminated the task of synthetic weather generation, the Simulink<sup>®</sup> weather modelling routines are left with the fairly standard task of converting values for global radiation on the horizontal into global radiation on an arbitrarily-oriented plane. This task is accomplished in a number of steps:

- 1) The hourly output file of Watgen must be in some way read into Simulink<sup>®</sup>.
- 2) The global radiation on the horizontal must be separated into beam and diffuse radiation on the horizontal.
- 3) The beam radiation in the plane of the array must be found from the beam radiation on the horizontal by trigonometry.
- 4) The diffuse radiation in the plane of the array must be found from the diffuse radiation on the horizontal using a sky model.
- 5) The beam, diffuse, and ground-reflected radiation are summed and form the output.

The approach was examined and the tester judged that it was reasonable. Only four minor comments arose from validation.

First, it would be helpful if the toolbox was capable of simulating a period longer than one year. Presently, the toolbox reads a TMY file of one year duration. Watgen is capable of generating data for a series of years; the PV Toolbox should be capable of utilizing this data.

Second, the beam ratio  $R_b$  is used to determine the ratio of beam radiation in the plane of the array to the beam radiation on the horizontal. The beam ratio is the cosine of the incidence angle divided by the cosine of the zenith angle. One danger of this approach is that  $R_b$  tends to “blow up” at the beginning and end of the day due to zenith angles approaching  $90^\circ$ . Often the methods used to determine the diffuse fraction from hourly data are insufficiently accurate: the product of the beam on the horizontal and  $R_b$  is unrealistically large at sunrise and sunset. The tester decided to wait until the verification stage to see if this results in a significant problem.

Third, because the simulation is based on a continuous-time approach, the output of the weather routines must be continuous. On the other hand, the input data is on an hourly time-scale. Furthermore, many of the methods implemented in the routines were developed for hourly data. This mixing of continuous output and discrete input may cause inaccuracies and complications. For example, in the existing method, the clearness index is calculated by dividing the terrestrial radiance on the horizontal by the extraterrestrial radiance on the horizontal. The latter can be calculated on a continuous basis, but the former is estimated by interpolating between hourly estimates of average irradiance. This raises the question of whether a correlation between diffuse fraction and clearness index for the hour can be used “as is” with this quasi-continuous approach. In general, the tester believes that it can, but there remains some uncertainty there.

Fourth, the Toolbox has not been updated to utilise the hourly temperature data generated by Watgen. Thus, the comments of Section 3.2.2 still apply.

### **3.5) White Box Verification of the Weather Modelling Routines**

Several problems were uncovered during white box verification of the revised weather modelling routines:

- 1) In the routine Solar Azimuth1, the second term in the solar azimuth angle calculation is multiplied by  $\pi/2$  when it should be multiplied by  $\pi$ .
- 2) In the routine Solar Azimuth1, the submodel for calculating the zenith angle has hard-wired parameters; i.e., a set of constants are passed to this block rather than the variables TZ, lat and long.
- 3) In the routine Solar Azimuth1, the variable  $C_1$  is not set to 1 when  $|\tan \delta / \tan \phi|$  is greater than 1, as required by Duffie and Beckman.
- 4) In the routine Horizontal Irradiance, hourly insolation data are read from a file generated by Watgen. Each hourly value is treated as if it were a measure of irradiance at the end of the hour, and then the irradiance is found by linearly interpolating among these hourly values. But the value generated by Watgen represents the insolation (i.e., the integral of irradiance) over the hour. For example,

the output of Watgen for 7 AM is the insolation for the hour of 6 AM to 7 AM, but the CEDRL toolbox treats this as an instantaneous measure of the irradiance at 7 AM.

Since the average irradiance over the hour is equal, by definition, to the insolation for the hour, the use of the insolation value as an irradiance is not especially problematic. On the other hand, using this average irradiance value as an estimate of the instantaneous irradiance at the end of the period does something akin to shifting the radiation profile into the future by 0.5 hours. It would be better to assume that the average irradiance (i.e., the insolation) is an estimate of the instantaneous irradiance at the middle of the hour.

A second issue with this approach is the uncertainty about when, at sunrise, the irradiance becomes non-zero and when, at sunset, it returns to zero. If, for example, the output of Watgen is 0 for the period of 4 AM to 5 AM but, say, 100 Wh/m<sup>2</sup> for the period of 5 AM to 6 AM, we know only that the irradiance stopped being non-zero at some time between 5 and 6 AM. Interpolating between the values of irradiance, we implicitly assume that irradiance goes non-zero at 5 AM. If we shift the radiation profile a half hour back in time to account for the problem mentioned above, we implicitly assume that irradiance goes non-zero at 4:30 AM. In this latter case we are definitely in error, while in the former case there is a very high probability that we are in error.

Generally the radiation at the beginning and the end of the day is not especially significant for photovoltaic system operation, and the accuracy of the toolbox is not likely to be limited by inaccuracy in the estimate of when irradiance goes non-zero or to zero. But this type of inaccuracy can set off a chain reaction of problems elsewhere in the routine. For example, the clearness index is calculated as the horizontal irradiance divided by the extraterrestrial irradiance on the horizontal. Inaccuracy in the estimate of the start and finish of day will lead to inaccuracy in the estimate of the clearness index, which will result in inaccuracy in the separation of the radiation into diffuse and beam parts. If multiplying by a large  $R_b$ , this may lead to significant errors in the estimate of radiation at the beginning and end of the day.

- 5) In the routine Omega\_s Sunset Hour Angle, there is no range checking to ensure that the argument to the arcosine function stays within the range  $-1$  through  $1$ . This may cause two problems. First, the output of the routine during polar day and polar night will depend on the output of the Simulink<sup>®</sup> arcosine function when its argument is out of range. This may have detrimental effects in routines that use this routine. Second, during polar day and polar night, Simulink<sup>®</sup> error messages will be displayed in the Matlab<sup>®</sup> window. This will probably slow down the simulation and will tend to hide more serious error messages appearing in this window.
- 6) In the routine Solar Azimuth1, there is no error checking to ensure that division by zero does not occur. When the sun is directly overhead, the zenith angle and its sine will be zero. This will cause division by zero in the calculation of the pseudo-azimuth angle. In addition, when directly on the equator, the calculation of the East-West hour angle will lead to division by zero.
- 7) In the routine Solar Azimuth1, there is no range checking to ensure that the argument to the arcosine function stays within the range  $-1$  through  $1$ . Thus when the magnitude of the declination exceeds the magnitude of the latitude, calculation of the East-West hour angle will lead to an error.

- 8) In the routine Hour to Solar Hour, the equation of time has not been included. This will result in errors of up to  $\pm 15$  minutes. This is a very minor problem.

### **3.6) Black Box Verification of the Weather Modelling Routines**

Black box verification consisted of testing individual blocks and sub-blocks of the routines using examples from Duffie and Beckman (1991) and other pathological or limiting cases. The goal was to find instances where the routines did not give realistic output or error messages. Rather than list all the tests, the problems that were revealed are listed below. These problems, along with those identified in white box testing, necessitated some changes to the routines, as described in Section 3.7. A final stage of black-box testing is described in Section 3.8.

- 1) The routines Solar Azimuth and Solar Azimuth1 are, once the problems identified in Section 3.5 have been rectified, accurate implementations of the method described in Duffie and Beckman. It was found, however, that this method gives incorrect values for the southern hemisphere: south of the equator it appears as though the azimuth angle of zero has been assigned to due north. On the equator itself, the values from this method are suspect, as alluded to by Duffie and Beckman.
- 2) In the routine Beam and Diffuse Irradiance, the correlation between the hourly clearness index and the diffuse fraction was implemented incorrectly. A saturation element was used to limit the diffuse fraction to a minimum of 0.165 as the hourly clearness index rose above 0.8. This approach presupposes that the quartic equation for diffuse fraction remains below 0.165 over the range (of clearness index) of 0.8 to 1. In fact, the equation rises significantly above 0.165 over this range.
- 3) A saturation element was placed at the input of each inverse trigonometric function to avoid out-of-range values. Despite these saturation elements, which should have limited the input to the inverse trigonometric functions to the range of  $-1$  to  $1$ , the trigonometric functions produced error messages indicating input out of range. This occurred when there was a very rapid transition from a large negative to a large positive input, or vice-versa. The saturation element was replaced by a function call, which incorporated error checking in the form of multiplication by expressions having relational operators. This solved the problem of out-of-range input.
- 4) The routine Tilt appeared to perform reasonably well under many conditions. There were, however, several aspects of its output that were unrealistic. At the beginning and end of the day, the insolation suggested by Watgen often approached or exceed the extraterrestrial. This is reasonable: the sky remains light after the sun has set, for example. But the Tilt routine calculates the clearness index (i.e., the ratio of terrestrial to extraterrestrial radiation) and uses this as input to the correlation determining the diffuse fraction. At the beginning and end of the day, most of the radiation on a horizontal surface is diffuse, but the high (sometimes infinite) clearness index combined with the correlation for diffuse fraction resulted in very low diffuse fractions. As a result, the beam radiation was unrealistically large. This tendency was exacerbated by the anisotropy index (calculated as the ratio of beam to extraterrestrial radiation): with high beam radiation, most diffuse is treated as circumsolar diffuse and is therefore multiplied by the beam ratio.

This problem manifested itself in several ways. First, surfaces facing east or west showed spikes of irradiance up to  $5 \text{ kW/m}^2$  at the beginning and end of the day, respectively. The high beam radiation multiplied by the high  $R_b$  resulted in unrealistic levels of beam radiation in the plane of the array. Second, at the zero-crossings of the extraterrestrial radiation, the anisotropy index made an abrupt transition between zero (its night-time value) and one. This caused an abrupt step in the radiation in the plane of the array. Third, because the Watgen output was shifted a half-hour into the future (see Section 3.5), the clearness index and consequently the beam radiation tended to be higher in the afternoon than the morning.

### 3.7) Changes

The problems identified in the white and black box investigations above necessitated a number of changes to the routines. These changes, described below, were made by the tester.

- 1) The method used in the routine Solar Azimuth1 was changed from that described in Duffie and Beckman (1991) to an alternative method described in the website <http://aurora.crest.org/basics/solar/angle/4.htm>:

$$\gamma_s = \cos^{-1} \left( \frac{\cos \theta_z \sin \phi - \sin \delta}{\sin \theta_z \cos \phi} \right)$$

where  $\gamma_s$  is the solar azimuth angle,  
 $\theta_z$  is the zenith angle,  
 $\phi$  is the latitude,

and  $\delta$  is the declination. The sign of the solar azimuth angle is set to match that of the hour angle. This method was validated and verified against examples from Duffie and Beckman (1991). Range checking and division by zero checking were implemented.

- 2) The hourly data values arising from the file generated by Watgen were shifted back in time one half-hour. In this way, the integrated values for the hour are used as estimates of the instantaneous value at the centre of the hour.
- 3) Range checking was implemented for the inverse trigonometric functions. Division by zero checking was also implemented.
- 4) The correlation for the diffuse fraction was modified such that values of the clearness index greater than 0.8 result in a diffuse fraction of 0.165.
- 5) The routine Tilt was changed rather substantially:
  - a) The hourly insolation generated by Watgen is no longer used directly. Rather, during initialisation the clearness index for the hour is calculated by dividing the Watgen generated hourly insolation by the integral of extraterrestrial radiation for the hour (see Eq. 1.10.4 in Duffie and Beckman (1991)). This clearness index for each hour is stored in an array, and then the instantaneous value of the clearness index is found by interpolation. The irradiance is calculated as the product of clearness index and the extraterrestrial radiation. For those hours which contain sunrise and sunset, the Watgen value is scaled by the fraction of the hour when

the sun is above the horizon. This helps to avoid excessively high hourly clearness indices. As a further precaution, the hourly clearness index is limited to unity.

There are a number of reasons for this change in approach. First, by using the integrated extraterrestrial and terrestrial radiation (rather than instantaneous extraterrestrial and interpolated terrestrial) more reasonable values of hourly clearness index tend to result. Second, calculating the clearness index for each hour and then interpolating between values permits the use of a correlation for diffuse fraction that is a function of hourly clearness index. As pointed out in Section 3.4, prior to this change the diffuse fraction was being correlated with a clearness index that was a strange admixture of instantaneous and integrated values. Third, this eliminates the issue of uncertainty about the time before sunrise and after sunset at which there is non-zero radiation: it is assumed that terrestrial radiation is zero whenever extraterrestrial radiation is zero. Obviously, this will mean that the simulation does not consider the diffuse radiation that occurs before sunrise and after sunset, but this is typically a very small fraction of the radiation incident on the array over the course of the day.

- b) The estimate of beam radiation in the plane of the array is limited by the beam radiation that would have passed through the ASHRAE clear sky standard atmosphere (see Figure 2.8.1 of Duffie and Beckman (1991) ). The product of the ASHRAE clear sky beam normal radiation (a function of zenith angle) and the cosine of the incidence angle for the plane of the array is used as an upper limit on the beam radiation.
- c) The beam part of radiation on the horizontal (i.e., the complement of the diffuse fraction) is limited by the beam radiation that would be incident on a horizontal surface according to the ASHRAE clear sky standard atmosphere. The maximum beam radiation incident on the horizontal according to this standard is subtracted from the total horizontal radiation. This establishes a floor for the diffuse fraction. The routine uses the maximum of this floor diffuse fraction and the diffuse fraction from the correlation with hourly clearness index.

These latter two changes greatly reduce the problem of radiation spikes at the beginning and end of day. They are not an ideal fix, however, because they limit the radiation in the plane of the array to an estimate of the maximum physically possible. But this is a biased estimate—it will tend to overestimate the beam radiation at the beginning and end of the day. Fortunately the first and last hours of the day are not typically responsible for the major portion of the radiation incident on a photovoltaic array so this solution should be acceptable. In any case, the output is much more realistic than prior to the changes.

Two minor criticisms of the existing routines were not rectified by the tester. First, the equation of time was not implemented, and thus the solar time may be out by up to 15 minutes. Second, the routine has not been updated to permit runs of multiple years of input data.

An additional shortcoming of the method as implemented is the time-consuming initialisation required to pass Watgen data into an array. The tester suspects that this can be made much quicker by taking advantage of the vector features of Matlab<sup>®</sup> and possibly by running the whole initialization procedure as an independent Matlab<sup>®</sup> script.

### 3.8) Final Black Box Testing

As a final, overall test of the weather routines, the irradiance in the plane of the array as modelled by the PV Toolbox was compared with the output of Watsun PV. This was done for various locations and various array orientations, described in the Table 3.1. In each case, Watgen was used to synthesize hourly data, and this was used as input to both the PV Toolbox and Watsun PV. Periods of 5 days were plotted (see Figures 3.8 through 3.14). For Entebbe, the latitude was entered as precisely zero in both Watsun PV and the PV Toolbox.

Location	Latitude	Orientation	Slope	Period
St. Hubert, Quebec	45.5 N	Due South	60°	January 1-5
St. Hubert, Quebec	45.5 N	Due South	60°	July 1-5
St. Hubert, Quebec	45.5 N	Due West	90°	March 20-25
Alert, Nunavut	82.5 N	Due South	60°	July 1-5
Entebbe, Uganda	0.1 N	Due East	90°	January 1-5
Nandi, Fiji	17.8 S	Due North	45°	March 20-25

Table 3.1 Final Test Cases for the Weather Routines

In general, the results are acceptably close. The largest discrepancies occur in the January St. Hubert simulation. On two days, the peak radiation according to the PV Toolbox is significantly higher than the peak according to Watsun PV. This is not necessarily an error on the part of the PV Toolbox; Watsun PV appears to produce some suspect output during this period. For example, on two days Watsun PV is unable to provide an estimate of the radiation for one or more hours, presumably due to a problem in its algorithm. On another day, Watsun PV predicts a peak radiation level of nearly 1200 W/m<sup>2</sup>. Given that the zenith angle at this point is roughly 66°, this seems very high: with the ASHRAE standard clear sky, the beam radiation would not exceed about 700 W/m<sup>2</sup>, requiring almost 500 W/m<sup>2</sup> of diffuse radiation. This would be unlikely given that a clear sky is assumed.

Significant discrepancies also occur in the March St. Hubert simulation. WatsunPV suggests higher values of irradiance at the end of the day for the vertical, west-facing array. On day 79, the output of the PV Toolbox is limited by the ASHRAE clear sky function; Watsun PV exceeds this limit. On the other hand, on days 82 and 83, the peak irradiance according to the PV Toolbox is about 100 W/m<sup>2</sup> greater than that for Watsun PV. It should be noted that although it appears that Watsun PV predicts a later sunset than the PV Toolbox, this is just an artifact of interpolating between hourly values.

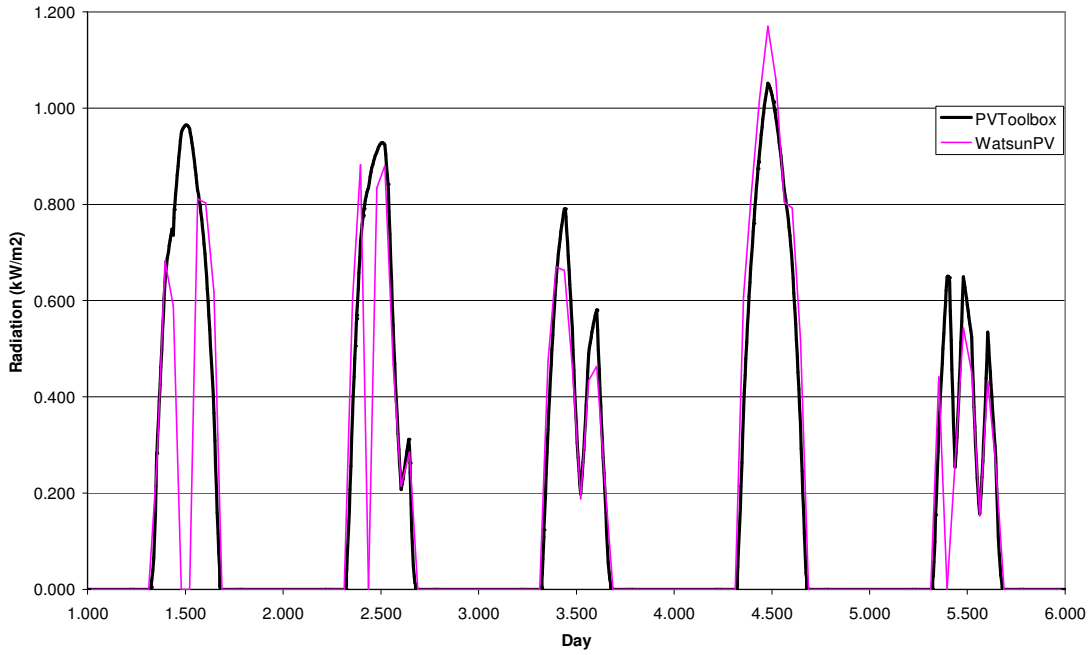


Figure 3.8 WatsunPV vs PVToolbox, January, St. Hubert, 60° Slope, 0° Azimuth

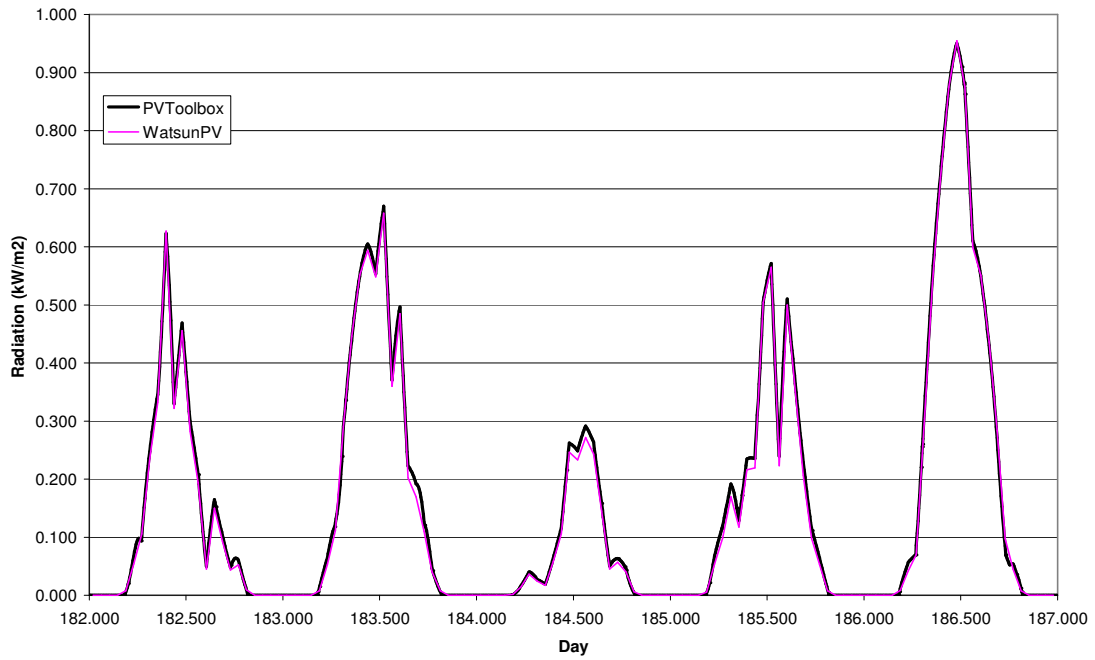
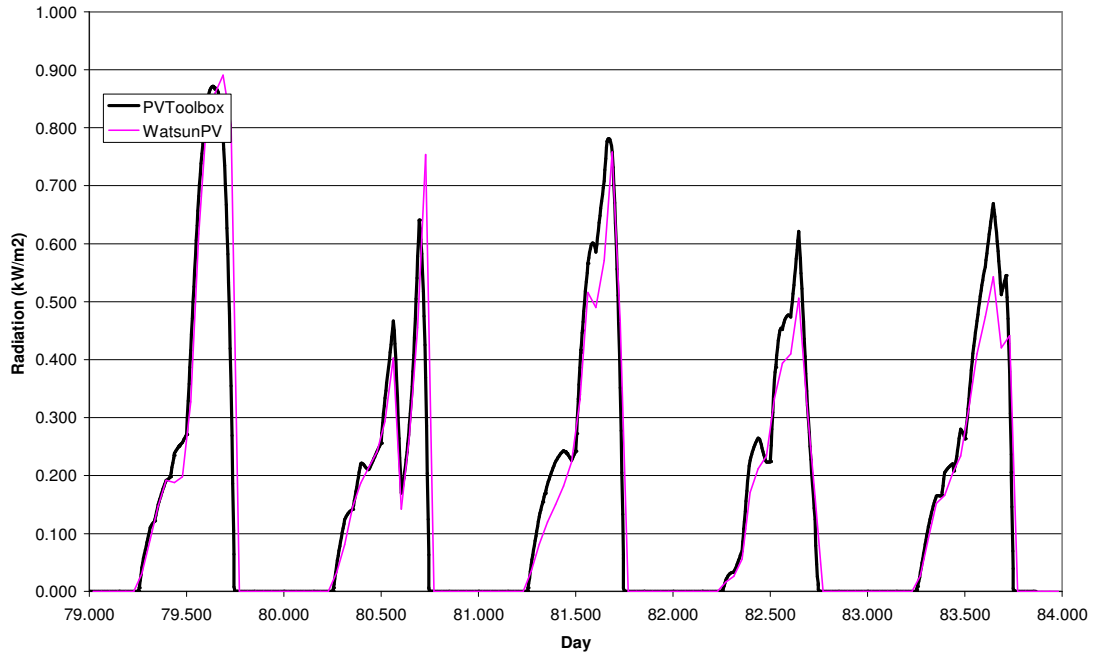
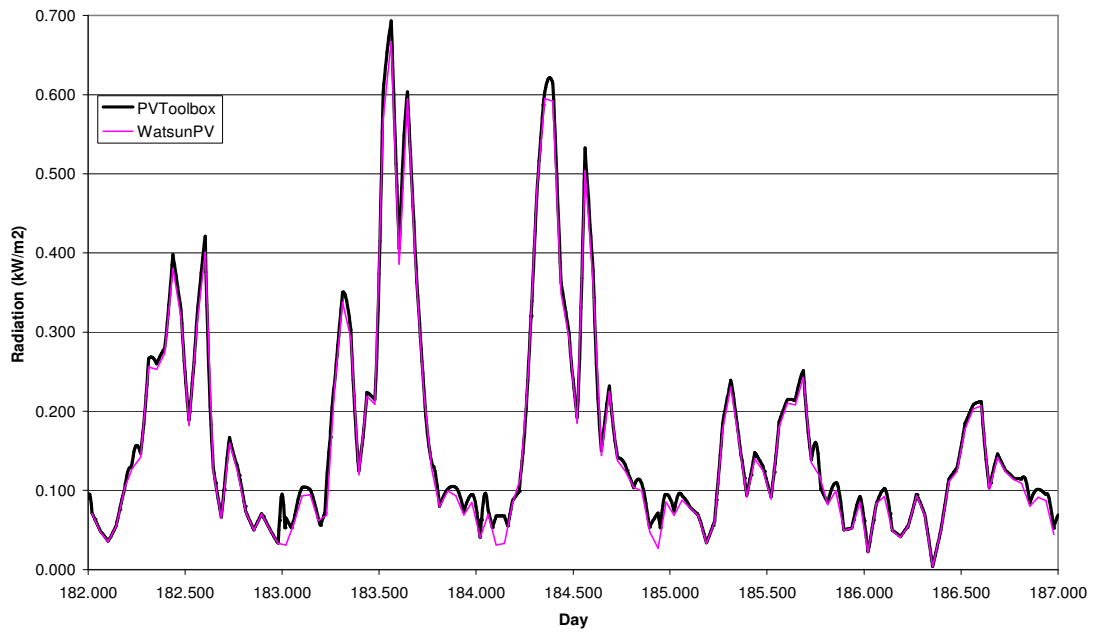


Figure 3.9 WatsunPV vs PVToolbox, July, St. Hubert, 60° Slope, 0° Azimuth



**Figure 3.10 WatsunPV vs PVToolbox, March, St. Hubert, 90° Slope, 90° Azimuth**



**Figure 3.11 WatsunPV vs PVToolbox, July, Alert, 60° Slope, 0° Azimuth**

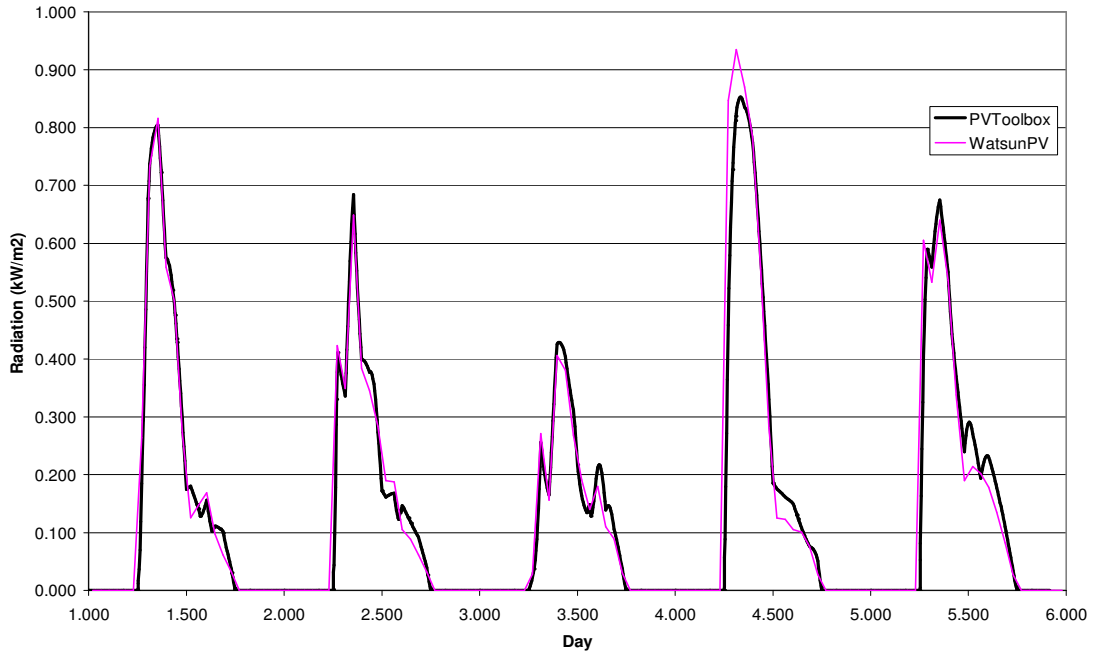


Figure 3.12 WatsunPV vs PVToolbox, January, Entebbe, 90° Slope, -90° Azimuth

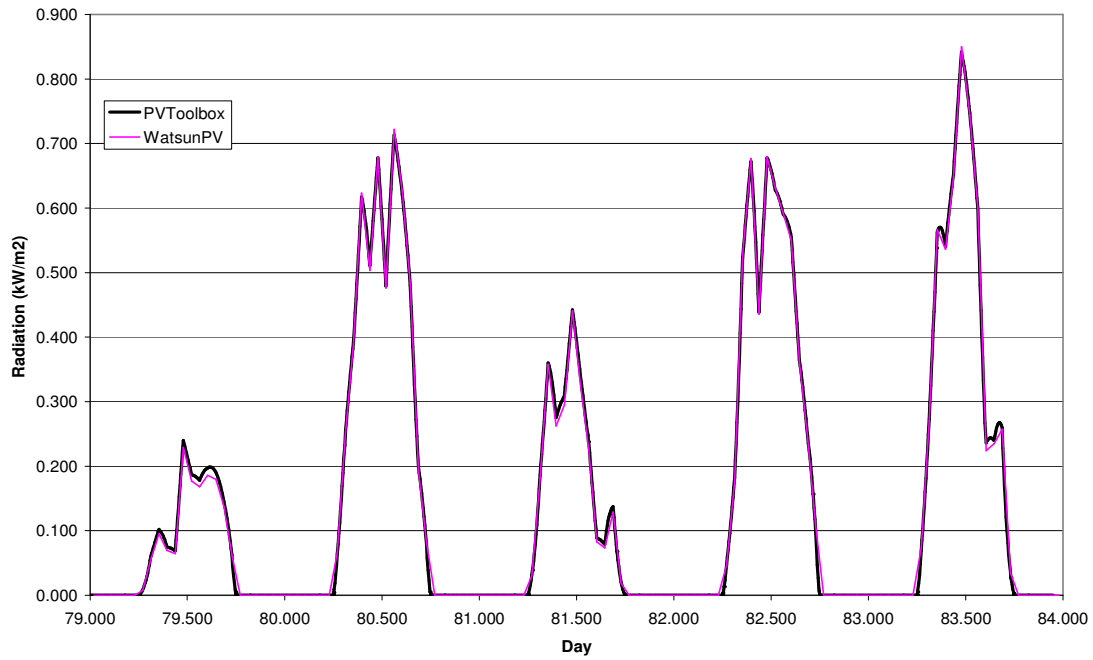


Figure 3.13 WatsunPV vs PVToolbox, March, Fiji, 45° Slope, 180° Azimuth (i.e. North)

#### 4) Photovoltaic Generator Modelling

The goal of the photovoltaic generator modelling is to predict the electrical output of an arbitrary photovoltaic array given the irradiance in the plane of the module and the

ambient air temperature. The electrical output can be given either in terms of a power, if the array is being used in conjunction with a maximum power point tracker, or a current, if the voltage is determined by other components in the circuit. It is assumed that the irradiance is uniform in the plane of the array.

There are three components to the photovoltaic model requiring validation:

- 1) A thermal model that calculates the module temperature given the ambient air temperature.
- 2) A “PV at MPPT” model that calculates the power output of a combination of PV array and maximum power point tracker, given ambient temperature and irradiance.
- 3) A “PV module” model that calculates the voltage of a PV array given ambient air temperature and irradiance.

#### 4.1) Photovoltaic Module Thermal Model

The photovoltaic module thermal model used in the CEDRL PV Toolbox is a well-accepted relation that appears in the literature (e.g., equations 23.3.1-3 in [Duffie et al., 1991]). It linearly relates the difference between module and ambient temperature to the irradiance in the plane of the array. It assumes the following conditions:

- a 1 m/s wind oriented toward the array as specified in the testing for the normal operating conditions temperature.
- the array being in the free air stream, i.e., rack-mounted.
- steady-state operation.

The wind speed and direction will generally be unknown for the simulation. This prevents the use of more accurate thermal models. The assumption of steady-state operation, constant over the hour, also introduces a small measure of error. Given no a priori knowledge about wind speed, the relation used is probably as accurate as any other that assumes steady-state operation.

It should be noted that the efficiency of the cells *at the operating point* is used in the relation. In the CEDRL PV Toolbox, the cell efficiency is assumed constant. Assuming a constant cell efficiency regardless of operating voltage and temperature will introduce a very small amount of error. For typical Siemens crystalline solar modules, for example, changing the efficiency from 14% to 7% raises the temperature by about 2°C according to this relation. This inaccuracy will likely be dwarfed by errors arising from ignoring the wind speed, equivalent sky temperature, etc. Alternatively, the actual module efficiency can be estimated, and this estimate refined by iteration to account for the inter-relation of temperature and efficiency.

#### 4.2) The Model for Photovoltaic Array at Maximum Power Point

The following equation is presently used to model the power output,  $P_{out}$ , of a maximum power point tracking circuit connected to a photovoltaic array:

$$P_{out} = \eta_{MPPT} \cdot P_{PV} \cdot \frac{G}{G_0} \cdot [1 + \beta(T - T_0)]$$

where  $\eta_{MPPT}$  is the efficiency of the maximum power point tracking circuit,

$P_{PV}$  is the nominal power output of the array at standard test conditions (STC),  
 $G$  is the irradiance seen by the array,  
 $G_0$  is the irradiance specified for STC,  
 $T$  is the operating temperature of the array,  
 $T_0$  is the operating temperature of the array specified for STC,  
 and  $\beta$  is the “neutered” voltage temperature effect coefficient, defined by

$$\beta = \frac{1}{V_{OC,0}} \cdot \frac{dV_{OC}}{dT} \cong \frac{1}{V_{OC,0}} \cdot \frac{V_{OC}(T_2) - V_{OC}(T_1)}{T_2 - T_1}$$

where  $V_{OC}$  is the open circuit voltage, the subscript  $0$  refers to standard test conditions, and  $T_1$  and  $T_2$  are two different operating temperatures.

The expression for  $P_{out}$  can be rewritten to make clear the effect of changes in temperature and irradiance:

$$P_{out} = \eta_{MPPT} \cdot \left( I_{MPPT,0} \cdot \frac{G}{G_0} \right) \cdot (V_{MPPT,0} \cdot [1 + \beta(T - T_0)])$$

where  $I_{MPPT,0}$  is the maximum power point current at STC,  
 and  $V_{MPPT,0}$  is the maximum power point voltage at STC.

A number of simplifications and assumptions need to be made in order to arrive at the above expression for  $P_{out}$ . Two of these may not be justified.

First, consider the effect of a change in temperature. The equation implies that  $I_{MPPT,0}$  does not change with temperature. This is a reasonable assumption;  $dI_{sc}/dT$  is typically of much smaller magnitude than  $dV_{OC}/dT$ , and  $dI_{MPPT}/dT$  is typically significantly smaller than  $dI_{sc}/dT$ . In the IV curves of Figure 4.1, it can be seen that a change of 100°C results in a very minor change in the maximum power point current but a major shift in the maximum power point voltage.

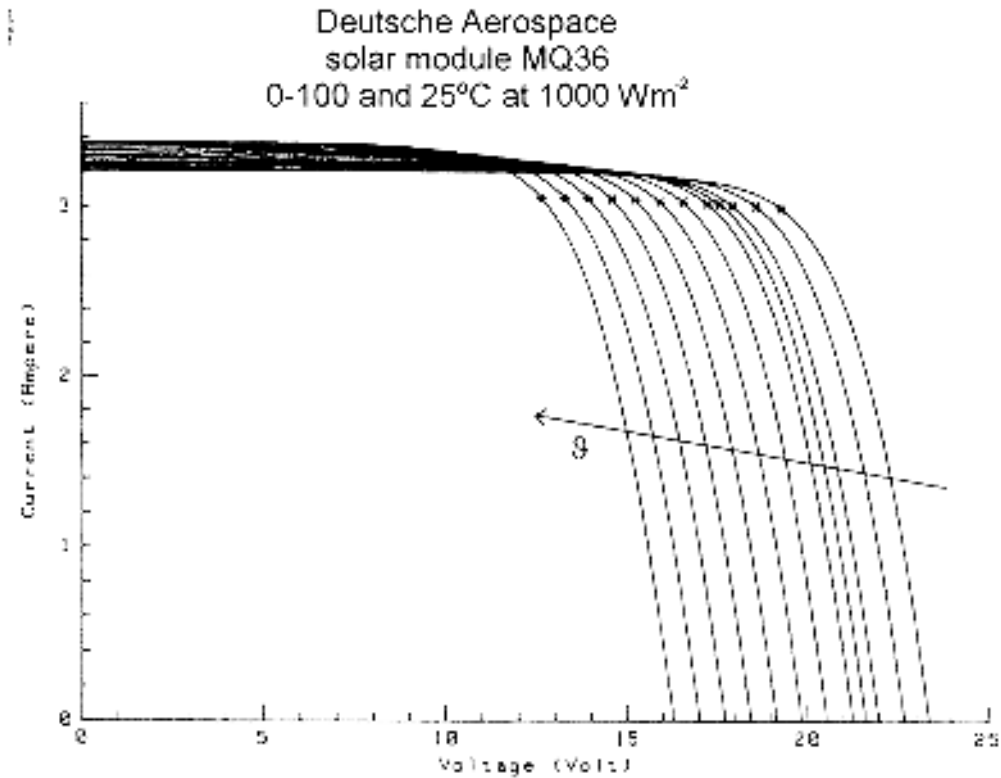


Figure 4.1 The Effect of Temperature on the Module IV Curve—The asterisks mark the maximum power points (from [Schmidt, 1995]).

On the other hand, the equation for  $P_{out}$  also implies that  $dV_{MPPT}/dT$  is less than  $dV_{OC}/dT$ . As can be seen in Figure 4.1, they are roughly the same. Thus  $\beta$ , which has been “neutered” by  $V_{OC,0}$ , should be multiplied by a factor of  $V_{OC,0}/V_{MPPT,0}$ . This result is derived formally in Equations 23.2.12 through 23.2.15 of [Duffie et al., 1991].

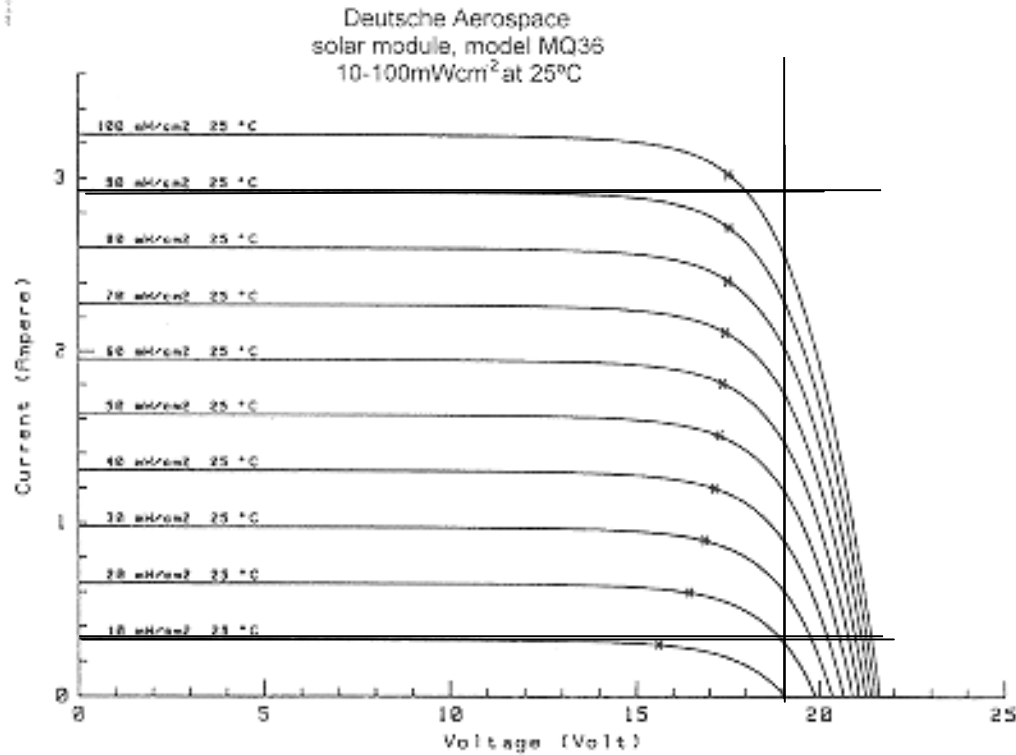


Figure 4.2 The Effect of Irradiance on the Module IV Curve—The asterisks mark the maximum power points (from [Schmidt, 1995]).

Next, consider the effect of a change in irradiance. The equation for  $P_{out}$  implies that  $I_{MPPT}$  is linearly related to the irradiance and that  $V_{MPPT}$  does not change with irradiance. Figure 4.2 shows that while the former assumption is reasonably accurate, the latter assumption is not: at low light levels, a pronounced decline in  $V_{MPPT}$  occurs. The IV curve translation equations detailed in [Anderson, 1996] and [Anderson, 1998] suggests that this decline can be estimated by dividing the voltage by a factor that changes with the natural logarithm of irradiance:

$$P_{out} = \eta_{MPPT} \cdot \left( I_{MPPT,0} \cdot \frac{G}{G_0} \right) \cdot \left( \frac{V_{MPPT,0}}{1 + \delta \ln\left(\frac{G_0}{G}\right)} \cdot \left[ 1 + \beta \frac{V_{OC,0}}{V_{MPPT,0}} (T - T_0) \right] \right)$$

where  $\delta$  is an empirical factor that can be found, given  $V_{OC}$  at STC and one other irradiance level, from

$$\delta = \frac{V_{OC,0} - V_{OC,1} \cdot (1 + \beta(T_1 - T_0))}{\ln\left(\frac{G_0}{G_1}\right) \cdot V_{OC,1} \cdot (1 + \beta(T_1 - T_0))}$$

where the subscript 0 denotes STC and the subscript 1 denotes the conditions at the second irradiance level. For the module shown in Figure 4.2,  $\delta$  is about 0.059; in [Anderson, 1998] a value of 0.085 is suggested for monocrystalline silicon photovoltaic

technology. When evaluating the above expression for  $\delta$ , one of the two irradiance levels should be  $300 \text{ W/m}^2$  or lower and the two temperatures should be as close as possible.

Even after taking into account the effect of irradiance on the maximum power point voltage, the function of maximum power versus irradiance appears essentially linear. The linear change in the maximum power point current dominates the non-linear effect in the voltage. This is observed in [Thevenard, 1999]. The same report observes that a straight line fit to the curve of maximum power between  $100$  and  $1000 \text{ W/m}^2$  does not pass through the origin; including the non-linear term above resolves this issue.

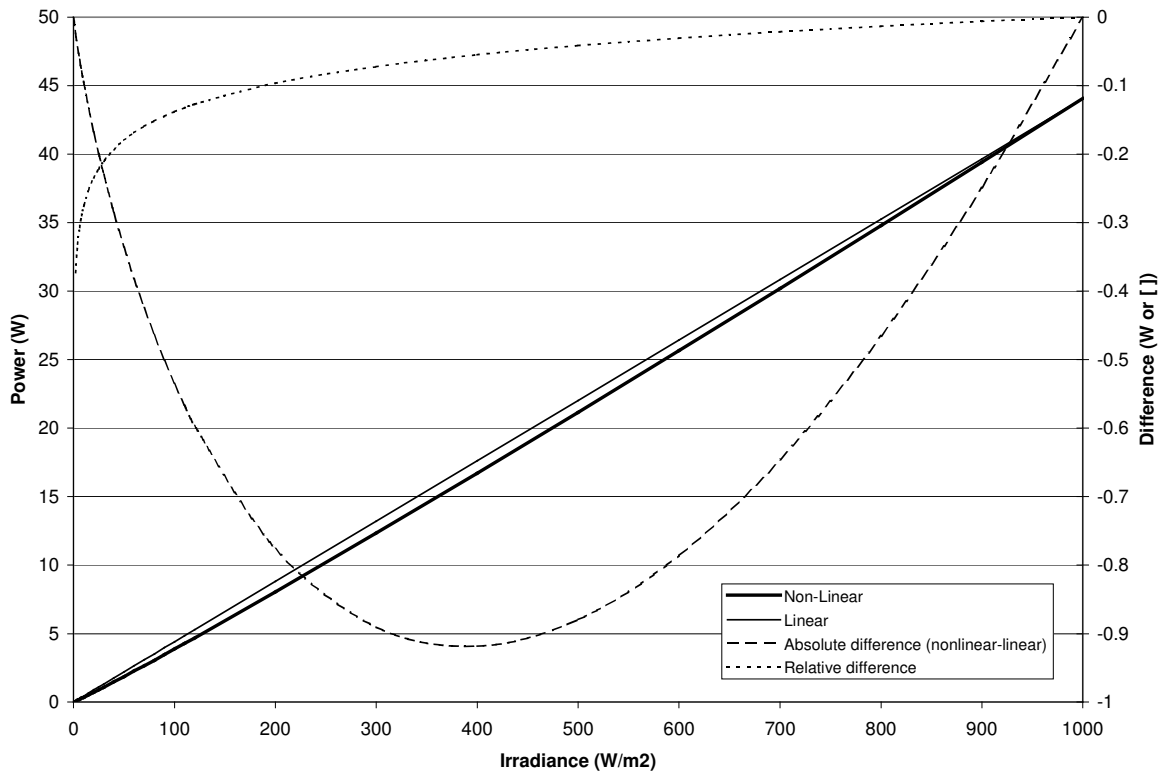


Figure 4.3 The Effect of Irradiance on Maximum Power: Linear versus Non-Linear

In Figure 4.3, a straight line between the origin and the module power at STC is compared with  $P_{out}$ , adjusted for the effect of irradiance on the maximum power point voltage. The modelled module is hypothetical, and it is impossible to say which relation is more accurate. The difference between the two could be reduced for irradiances above, say,  $100 \text{ W/m}^2$ , by not constraining the linear expression to pass through the origin (i.e., by fitting the curve as in [Thevenard, 1999]). In general, however, there will be insufficient data to do this, and the origin is an obvious choice of second point on the power versus irradiance curve.

Thus, compared with the behaviour of an ideal module, there are two suspect simplifications in the original expression for  $P_{out}$ . First,  $\beta$  has been “neutered” by  $V_{oc}$  instead of  $V_{MPPT}$ . Second,  $V_{MPPT}$  is assumed to be constant with irradiance, whereas there is a strong indication that it is not. The other assumptions implicit in the expression are reasonable.

In terms of the behaviour of real, as opposed to ideal, modules, there may be further inaccuracies in the expression for  $P_{out}$ . In particular, the efficiency of photovoltaic modules often declines at low irradiance levels: the fill factor deteriorates below, say, 300 W/m<sup>2</sup>. The extent to which this occurs varies from one module type to the next, is not documented in the specifications of most modules, and is not considered here. It is probable, however, that for certain modules this will cause the dominant error when using the above expression for  $P_{out}$ .

### 4.3) The PV Module Model

A one diode equivalent circuit model is used to model the current of the PV module given an operating voltage, temperature, and irradiance level. The locus of (V,I) points at STC is described by an equation, and then this locus is shifted left or right to account for changes in temperature and up or down to account for changes in irradiance and/or temperature.

The expression for the locus of (V,I) points at STC has been determined to be accurate in terms of the following:

- 1) The curve crosses the voltage and current axes at the specified  $I_{sc}$  and  $V_{oc}$ .
- 2) The curve includes the specified point ( $V_{mp}$ ,  $I_{mp}$ ).
- 3) The maximum power point of the curve is very close to the specified point ( $V_{mp}$ ,  $I_{mp}$ )
- 4) To the eye the curve appears quite reasonable—i.e., it exhibits the tendencies of a real module's IV curve.

The model's output is unacceptable under certain conditions, however. The current of the PV device,  $I_{new}$ , is calculated by:

$$I_{new} = I_{sc,0} \frac{G}{G_0} + I_{sc,0} \alpha (T_c - T_0) - I_{sc,0} C_1 \left[ \exp \left( \frac{V_{new} - V_{oc,0} \beta (T_c - T_0)}{C_2 V_{oc,0}} \right) - 1 \right]$$

where  $I_{sc,0}$  is the short-circuit current at STC in Amperes,

$G$  is irradiance in kW/m<sup>2</sup>,

$G_0$  is irradiance at STC in kW/m<sup>2</sup>,

$\alpha$  and  $\beta$  are the temperature coefficients for  $I_{sc}$  and  $V_{oc}$ , respectively,

$T_c$  is the cell temperature, in degrees Celsius,

$T_a$  is ambient temperature, in degrees Celsius,

$C_1$  and  $C_2$  are positive constants,

$V_{new}$  is the voltage seen at the PV device terminals, in volts,

and  $V_{oc,0}$  is the open-circuit voltage at STC, in volts. Examination of this expression for current reveals two problems:

- 1) Even when the cell temperature is equal to the STC temperature, non-zero current can occur when there is no irradiance. When a battery is connected to the module,  $V_{new}$  will be equal to the battery voltage. This will result in a small but non-negligible negative current output.
- 2) When the cell temperature is not equal to the STC temperature, non-zero current can occur when there is no irradiance due to the  $\alpha$  and  $\beta$  correction terms.

Both of these problems can be circumvented if the  $\alpha$  and  $\beta$  correction terms are limited in magnitude such that they never exceed the first term on the right hand side. The

expression will still not be perfectly accurate at very low irradiance levels, but at least the current will be forced to zero when the irradiance is zero.

The model has other shortcomings, as well. For one, it assumes that the shunt resistance of the module is infinite. This is a reasonable assumption for most commercially available crystalline modules, but will be inaccurate for any module that has a pronounced slope in its IV curve at low voltages (e.g., some amorphous silicon modules). Another shortcoming of this model is that it does not account for deteriorating efficiency at low irradiance levels, as discussed in the previous section of this report.

The translation procedure accounts for the shift in the IV curve that occurs with changes in temperature (compare Figures 4.1 and 4.4) and irradiance (compare Figures 4.2 and 4.5) but fails to reproduce the subtle change in the shape of the IV curve that occurs when irradiance changes. The intersecting vertical and horizontal lines that have been superimposed on Figures 4.2 and 4.5 make this evident.

Note, however, that the model is significantly in error only at voltages at or above the “knee” of the curve. Thus, the model will tend to be inaccurate only when battery charging systems use modules of 30 or fewer crystalline cells, when very high charge currents are used, or when module temperatures are very elevated. These issues are not central to the planned hybrid system research, so the model can be considered acceptable.

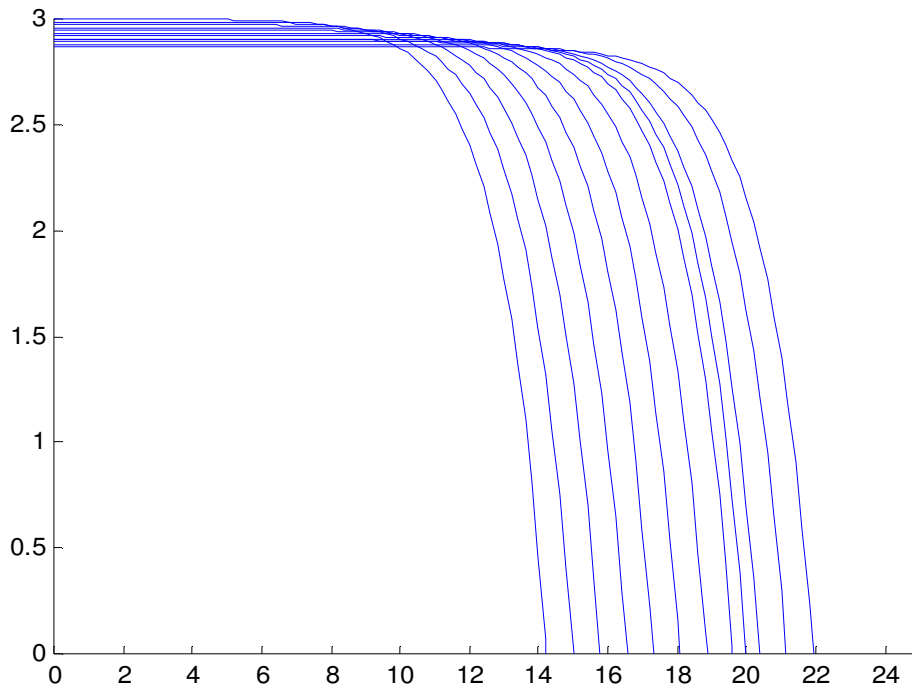


Figure 4.4 Modelled IV Curves at 1000 W/m<sup>2</sup> and Cell Temperatures of 0 Through 100°C and 25°C (Matlab<sup>®</sup> model implemented by tester)

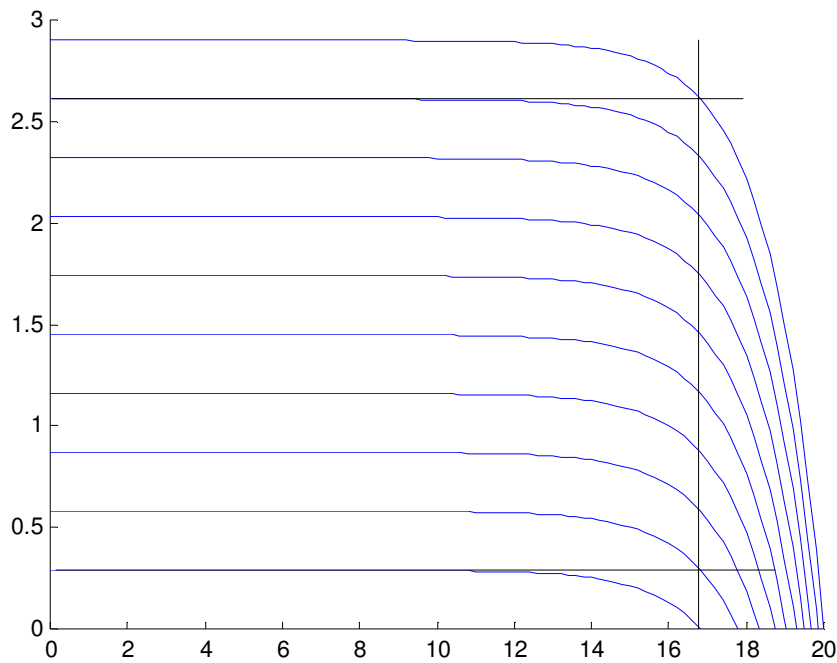


Figure 4.5 Modelled IV Curves at 25°C and Irradiance from 100 to 1000 W/m<sup>2</sup> (Matlab<sup>®</sup> model implemented by tester)

#### 4.4) Changes to the Models Following Validation

The concerns voiced in the sections above were addressed through changes to the model. The model for the photovoltaic array at maximum power point was changed in the two ways suggested, such that output power includes a  $\delta$  term and  $\beta$  is neutered by  $V_{mp}$ , as shown in the final expression for output power above. The model for the photovoltaic module was modified such that the magnitude of the  $\alpha$  and  $\beta$  correction terms are limited and thereby the current is forced to zero at zero irradiance.

#### 4.5) Verification of the Model for Photovoltaic Array at Maximum Power Point

A white box examination of the model, implemented in Simulink<sup>®</sup> revealed no problems. Following this, the correct implementation of the model was verified in four black box tests.

In the first test, the irradiance signal was a ramp from 0 to 1400 W/m<sup>2</sup> and the ambient air temperature was a constant. The power output predicted by the model was a reasonably straight line from the origin to a maximum of approximately 70 to 100 W (depending on the constant used for temperature), which was reasonable for the input parameters. Three ambient temperatures were tried: -10, 20, and 50°C. The power output decreased with rising ambient air temperature, and the decrease at a given irradiance level was approximately the same going from -10 to 20°C as from 20 to 50°C. This test established that the model functioned over an acceptable range of input parameters and had the general behaviour expected of it.

In the second test, the parameters for the model were taken from Examples 23.2.1 and 23.3.1 of [Duffie and Beckman, 1991]. The inputs to the model were an ambient air temperature of 40°C and an irradiance level of 920 W/m<sup>2</sup>; these correspond to the conditions of Example 23.3.1. Using an MPPT efficiency of 100%, a module efficiency of 14%, and a  $\delta$  (i.e., coefficient for how the power output changes with the natural logarithm of irradiance) of 0.085, the Simulink<sup>®</sup> model gave an output of 32.64 W. According to Duffie and Beckman (1991), the true output is 32.1W, a difference of under 2%. Changing the cell efficiency to 8.2% (the actual operating efficiency in this case) resulted in an output of 32.27 W. Following this,  $\delta$  was changed to 0.054, which was calculated from the output of the Duffie and Beckman (1991) model at 1000 and 200 W/m<sup>2</sup>. The output rose to 32.36 W. This test showed that at high temperatures and irradiance levels, using the default efficiency and  $\delta$  parameters for monocrystalline silicon modules, the output of the model was within 2% of the output of a more sophisticated model. Accuracy can be improved by adjusting the efficiency and  $\delta$  parameters.

In the third test, the Duffie and Beckman (1991) equivalent circuit model was implemented in Excel, tested against data given in Duffie and Beckman (1991) and then used to test the Simulink<sup>®</sup> model at low irradiance levels. The default monocrystalline silicon efficiency and  $\delta$  parameters and an MPPT efficiency of 100% were used. The ambient air temperature was set to 0°C and the irradiance to 200 W/m<sup>2</sup>. The model output was 8.46 W. According to the model of Duffie and Beckman (1991), the output should be 9.33 W, a difference of -9%. Changing the efficiency to 10.9%, the operating efficiency according to the Excel model, lowered the Simulink<sup>®</sup> model output to 8.45 W. Changing  $\delta$  to 0.054 raised the Simulink<sup>®</sup> model output to 8.84 W, thus reducing the error to -5%.

The above three tests show that the Simulink<sup>®</sup> model gives reasonable values for PV module output power. Using the default parameters for module efficiency and  $\delta$  is acceptable. The model deviates from the Duffie and Beckman (1991) equivalent circuit model at low irradiance levels. Since it predicts power output lower than the equivalent circuit model, which ignores eroding fill factors at low light levels, it may be, in fact, more representative.

In the fourth test, miscellaneous aspects of the Simulink<sup>®</sup> model were examined. The tracker efficiency was lowered from 100% to 50% and it was confirmed that the power output halved. The maintenance interval was set to 0.1 years and the lifetime to 0.5 years. Running the simulation for 8760 hours showed an O&M vector of 0 fuel costs, 10 maintenance visits, 0 overhauls, and 2 replacements. These are good indications that the model is implemented correctly.

#### **4.6) Verification of the Model for the PV Array**

White box examination of the model revealed two minor problems. First, in the exponential term of the expression for current, the sign of the term that includes  $\beta$  was positive but should have been negative. This was corrected. Second, an undocumented part of the model that was supposed to calculate the open circuit voltage corresponding to the given module temperature and irradiance was incorrect. This part of the model was subsequently removed.

Four black box tests established the correct implementation of the model. In the first, the irradiance was held constant at  $1000 \text{ W/m}^2$  while the cell temperature was varied from  $0$  to  $100^\circ\text{C}$  in  $10^\circ\text{C}$  increments ( $25^\circ\text{C}$  was also used). Since the input to the model is the ambient air temperature, the module thermal model was implemented in Excel and used to calculate the ambient temperature corresponding to the target cell temperature. The model parameters describing the PV module were taken from Examples 23.2.1 and 23.3.1 in Duffie and Beckman (1991). The output of the Simulink<sup>®</sup> model was fed to an Excel worksheet where it was graphed (see Figure 4.6). This can then be compared with Figure 4.4, which was generated using identical inputs and the same model, but implemented in Matlab<sup>®</sup> by the tester. The output appears to be identical.

In the second black box test, the cell temperature was held constant at  $25^\circ\text{C}$  while the irradiance was varied from  $100$  to  $1000 \text{ W/m}^2$  in  $100 \text{ W/m}^2$  increments. Once again, the Excel temperature model was used to calculate the ambient air temperature corresponding to the target cell temperature of  $25^\circ\text{C}$ . The graph of the Simulink<sup>®</sup> model output is shown in Figure 4.7. This should be compared to Figure 4.5, which was generated by the tester using a Matlab<sup>®</sup> implementation of the model. The output appears to be identical.

In the third black box test, the model was used to calculate the current for the module and conditions described in Example 23.3.1 of Duffie and Beckman (1991). The model of Duffie and Beckman (1991) predicts a current of  $2.49 \text{ A}$ ; the Simulink<sup>®</sup> model predicts  $2.56 \text{ A}$ . This is acceptably close. Furthermore, it was verified that under standard test conditions the model predicts a current equal to  $I_{sc}$  when the voltage is set to  $0$  and a current of  $0$  when the voltage is set to  $V_{oc}$ .

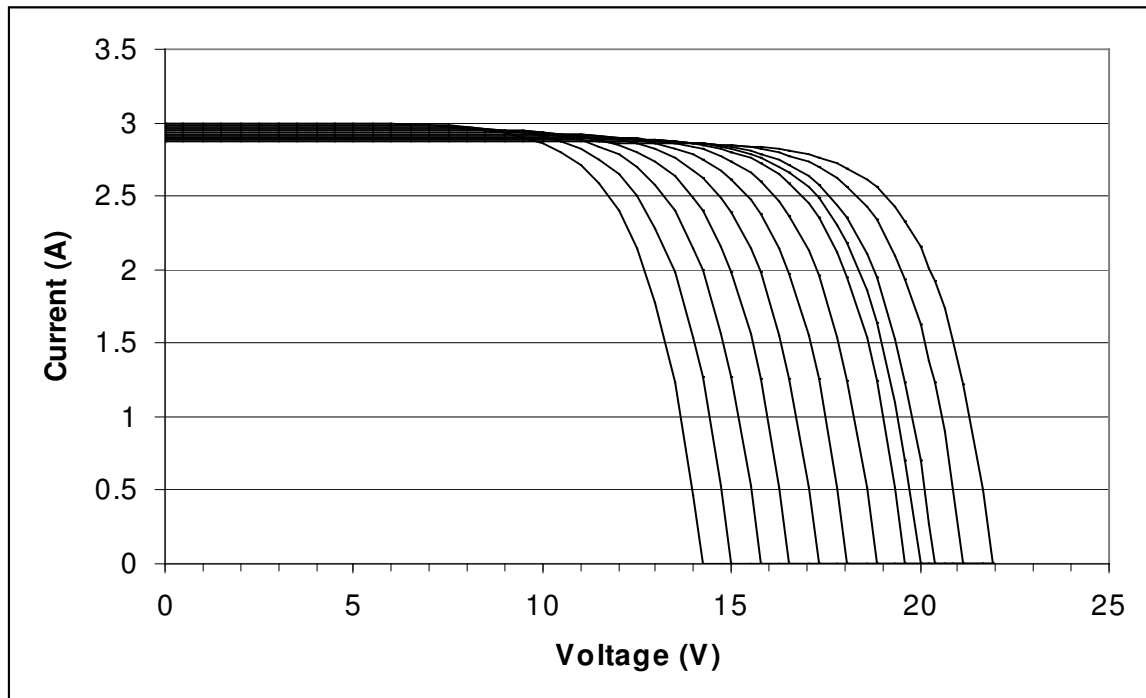


Figure 4.6 Modelled IV Curves at  $1000 \text{ W/m}^2$  and Cell Temperatures of  $0$  Through  $100^\circ\text{C}$  and  $25^\circ\text{C}$  (Simulink<sup>®</sup> Model)

In the fourth test, the maintenance interval was set to 0.1 years and the lifetime to 0.5 years. Running the simulation for 8760 hours showed an O&M vector of 0 fuel costs, 10 maintenance visits, 0 overhauls, and 2 replacements. These are good indications that the model is implemented correctly.

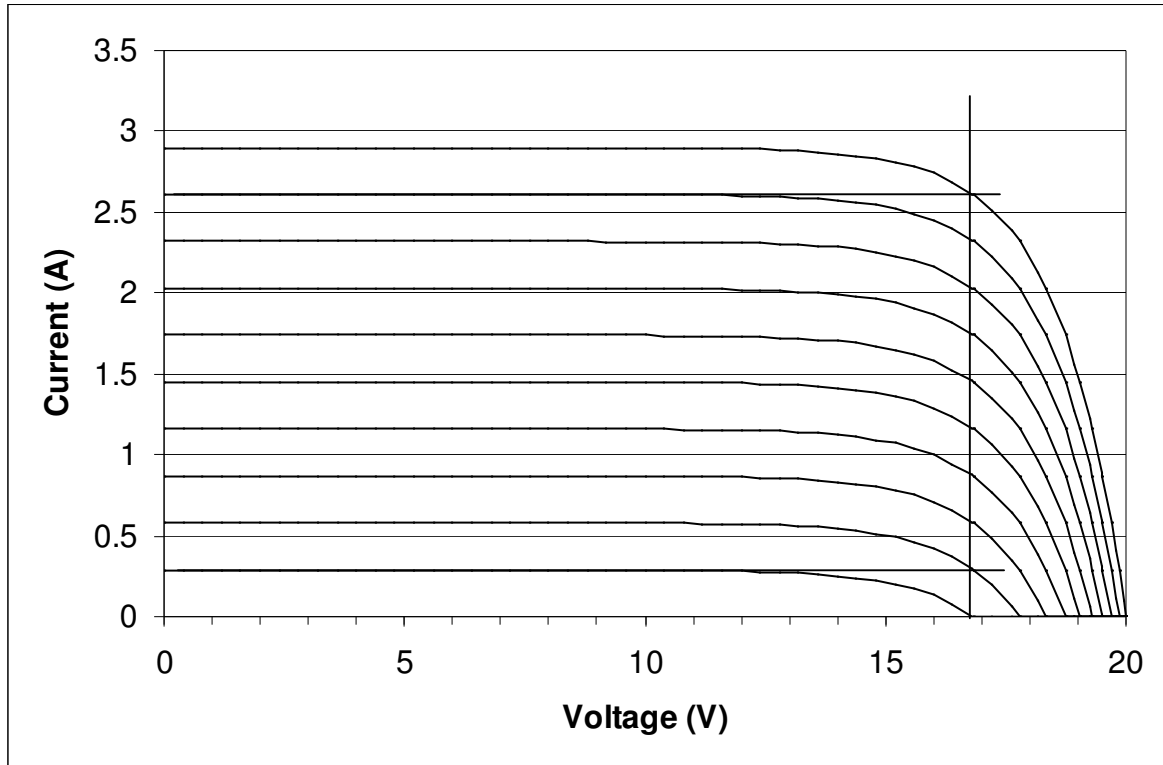


Figure 4.7 Modelled IV Curves at 25°C and Irradiance from 100 to 1000 W/m<sup>2</sup> (Simulink<sup>®</sup> Model)

### 5) Thermal Mass and Fuel Reservoir Model

The CEDRL Hybrid System modelling program aims to optimize energy flows within PV-battery-genset hybrid systems. Energy flows are not limited to electricity; rather, they include the flow of heat between components and the environment. Because temperature is an important parameter in the operation of the genset and the battery, the way that these heat flows are managed may have a significant impact on overall system efficiency, reliability, and maintenance requirements.

The components which need to be modelled are the genset, the battery, the fuel tank and the equipment enclosure (the photovoltaic module thermal model being treated separately above).

These models must satisfy two objectives:

- 1) The temperature of the component needs to be known as a function of time.

- 2) The heat flow between the component and its environment needs to be known as a function of time.

Two models have been developed: a fuel reservoir thermal model, and, for all other components, a thermal mass model.

### 5.1) Thermal Mass Model

The thermal mass model is a lumped parameter model: the entire thermal mass is characterised by a single node and it is assumed that the component is isothermal. The heat capacity of the component is assumed to be constant with temperature:

$$Q = \frac{dq}{dt} = -mc_p \frac{dT}{dt}$$

where  $Q$  is the rate of heat transfer from the component to the environment, typically in W,  
 $q$  is the sensible heat content of the component,  
 $t$  is time,  
 $m$  is mass,  
 $c_p$  is the specific heat capacity of the component,  
and  $T$  is the temperature of the component.

The net heat flow out of the component is assumed to occur at a rate proportional to the difference in temperature between the component and the ambient air:

$$Q = \frac{1}{R}(T - T_{amb})$$

where  $R$  is an overall resistance to heat transfer,  
and  $T_{amb}$  is the ambient air temperature.

Combining these two equations yields an ordinary differential equation:

$$\frac{dT}{dt} = \frac{1}{Rmc_p}(T_{amb} - T)$$

Because the difference between the ambient and the component temperature will, in general, change relatively slowly, it introduces minimal error to numerically integrate  $dT/dt$  with respect to time to solve for  $T$ . This is the approach used in the CEDRL PV Toolbox, which is implemented in Simulink®, a simulation software that steps through time. Alternatively, the closed form solution over a time step where the ambient air temperature is assumed constant is:

$$T = (T_0 - T_{amb})e^{\frac{-t}{Rmc_p}} + T_{amb}$$

where  $T_0$  is the component temperature at the beginning of the time step.

### 5.2) Fuel Reservoir Thermal Model

The fuel reservoir thermal model is essentially the same as the thermal mass model except that the specific heat capacity is no longer considered independent of temperature.

According to Perry (1997), the specific heat capacity of fuel oil can be estimated to within 2 to 4% of measured values by:

$$c_p = \frac{1.685 + (0.039T)}{\sqrt{s}}$$

where  $s$  is the specific gravity of the fuel at 15°C with respect to water at the same temperature. For fuel oil #2 (commonly known as diesel oil), this is roughly 0.80 to 0.87 according to the DieselNet Technology Guide (2001).

### 5.3) Application of the Models

The models are based on standard relations for heat transfer, and as such do not require investigation. What can be questioned is whether the assumptions that underlie the lumped parameter approach are reasonable. In general, the approach appears acceptable, with the following limitations and concerns:

- 1) The heat transfer between the component and the environment is assumed to be proportional to the temperature difference between the two. This does not allow for heat transfer by radiation, which is proportional to the difference between the fourth power of the temperature of the component and the fourth power of the equivalent black-body temperature of the environment. In general, heat transfer by radiation will only become significant when the difference in temperature between the environment and the component is relatively large, perhaps 10°C or larger. This situation will only occur when either the component has a major internal source or sink of heat (e.g., the heat generated during genset operation) or when the ambient temperature changes rapidly compared with the time constant of the component (e.g., the component is not in an enclosure.)
- 2) The most error-prone part of the existing approach is the calculation of  $R$ , the resistance to heat transfer. In many cases, heat transfer between the component and the environment will be dominated by natural convection. Thus, calculating  $R$  requires evaluating  $h_c$ , the convective heat transfer coefficient. At best, the convective heat transfer coefficient will be a reasonable approximation of reality. It should be noted that determining  $h_c$  can be a fairly involved calculation, prone to human error.
- 3) The convective heat transfer coefficient is typically a nonlinear function of the difference between the surface temperature and the ambient air temperature. Thus  $R$  is not constant, as assumed in the above models. If the range of values taken by the temperature difference is very small, using a constant for  $R$  will not cause large errors. Thus, as long as the component stays within close to the ambient air temperature, the approach is valid.
- 4) When the inlet and exhaust ports of an equipment enclosure are open, or when the genset radiator fan is operating, significant air currents may circulate within the equipment enclosure. Heat transfer by forced convection may therefore dominate heat transfer by natural convection. In general, the distribution of air currents within an equipment enclosure will be unknown, and therefore predicting the rate of forced convection will be impossible.
- 5) The isothermal assumption will be suspect when there is a significant heat source or sink within the component. This will be the case, for example, when the genset is operating.

In general, therefore, the approach will be valid except when:

- The genset is operating or
- The enclosure is poorly insulated or the temperature of the air around the component is closely tied to the outside air temperature.

Given that the existing approach will not be accurate when the genset is operating, it must be decided whether it is necessary to accurately model the temperature of components during genset operation and cool down. While it is important that the air temperature in the enclosure not reach very high levels, this appears to be more a question of specific equipment design, and not system modelling.

For system modelling, it is probably sufficient that the temperature of the components be accurate to within 5°C over the long run. That is, it should be acceptable that the temperature is significantly in error during and immediately following genset operation, as long as the errors have returned to within 5°C or so within, say, half a day of genset shut down. Furthermore, it should be noted that cold temperatures are most critical from the system modelling perspective because the control system will start the genset when its temperature drops below a certain level. Thus errors during operation and cool down, when temperatures will be high, should not be critical.

Accurate modelling of the net heat gain within the equipment enclosure during genset operation is key. With this accurately accounted for, the long term effect of genset operation on the temperature of the components within the enclosure can be determined.

It can be assumed that during genset operation, the genset temperature and the air temperature within the enclosure will reach steady-state. If we assume that the enclosure is designed in such a way that its ambient air temperature does not change greatly when the genset is in operation, the task at hand is considerably simplified: the heat transfer processes occurring during operation need not be accounted for, their net effect being zero. In other words, regardless of how long the genset has been operated, its effect on the long term temperature of the components in the enclosure will be fully characterized by 1) the net heat transferred to the coolant reservoir during operation, 2) the steady-state operating temperature of the genset and 3) the heat capacity of the genset. This may afford a simplified approach to thermal modelling.

If it is decided that the thermal models only need predict the temperature to within, say 5°C, and that inaccuracies during and immediately after genset operation are not important, then it may simplify matters to lump all the contents of the enclosure together. That is, the thermal mass of the genset, batteries, fuel tank, coolant reservoir, controls, etc. (assuming that they are all in the same enclosure) would be lumped together and assumed isothermal. If the enclosure is at least minimally insulated, the isothermal assumption should not result in significant additional error. Furthermore, under these conditions the limiting heat transfer process will probably be the conduction across the enclosure wall. This is much more simply evaluated than the convective heat transfer coefficient.

Of course, this simplification is not necessary: the existing component models can be linked through the thermal mass of the air in the enclosure to achieve the same effect. But it seems unlikely that this more complex approach would yield significantly more accurate results: differences in component temperatures will probably result principally

from thermal gradients within the enclosure (e.g., cold air near the walls and floor) that are not accounted for by either approach.

## **6) Inverter Model**

### **6.1) Validation**

The objective of the inverter model is to determine the DC input power required for a given level of AC output demanded by the load.

The inverter model expresses DC input power as a quadratic function of AC output power. This approach assumes that inverter power losses consist of constant losses (self-consumption), losses linearly related to output power (voltage drops) and losses related to the square of output power (ohmic losses) [Jantsch et al., 1992]. Rather than attempt to validate this assumption directly, the model was tested by examining whether it could accurately generate the efficiency curves of a selection of inverters.

Efficiency curves from 11 inverters were taken from the literature and manufacturer's data sheets. For each curve, 8 to 14 points along the curve were used to describe the relationship between input and output power. Excel was used to determine the coefficients for the quadratic equation that, in a least-squared sense, best fit this relationship. Then the efficiency curve was graphed based on the quadratic equation and these coefficients. The results are shown in Figures 6.1 through 6.11.

For the inverters in Figures 6.1 through 6.7, data were taken from the manufacturers' specification sheets; the inverter in Figure 6.8 was measured by Haeberlin et al. (1995); the inverter in Figure 6.9 was measured by Haeberlin et al. (1997); the inverter in Figure 6.10 was measured by Oldenkamp et al. (1997); and the inverter in Figure 6.11 was measured by Wilk and Schauer (1997). This set of inverters includes grid-tied models; although the hybrid system research of CEDRL is more likely to be concerned with stand-alone inverters, the efficiency curves of the two should be sufficiently similar to permit validation of the approach.

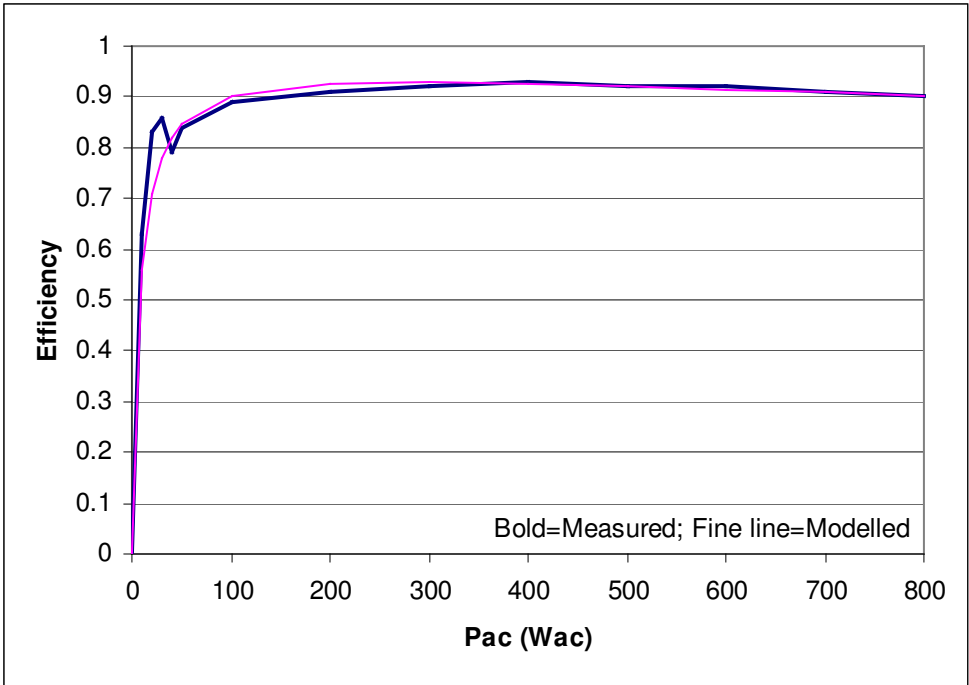


Figure 6.1 Efficiency of MLT Drives MLT800t24 24V Twin Inverter (800 W)

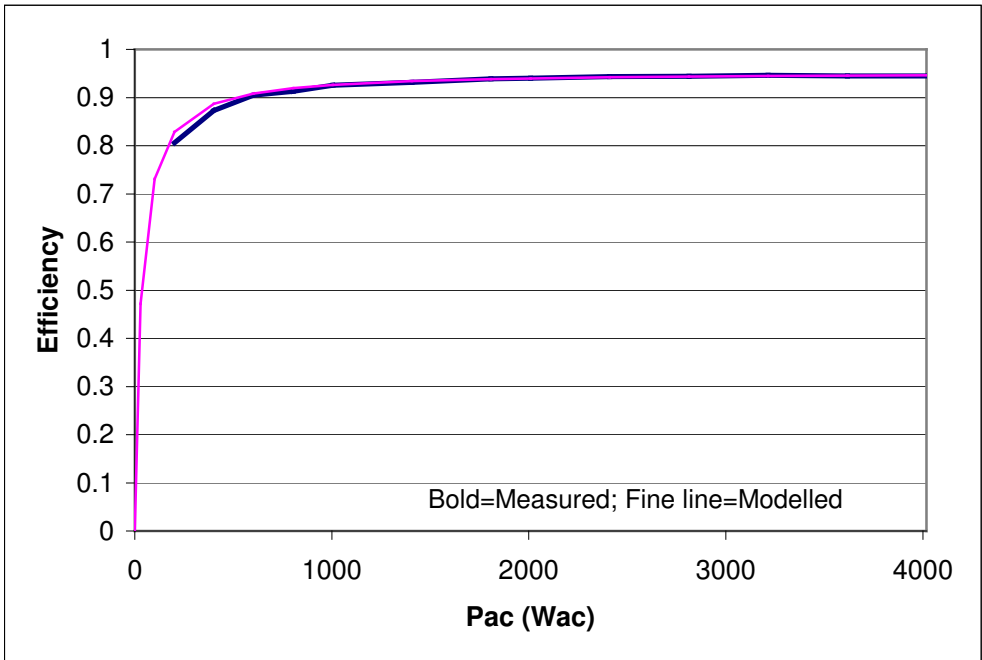


Figure 6.2 Efficiency of Omnion Series 2400 (4kW)

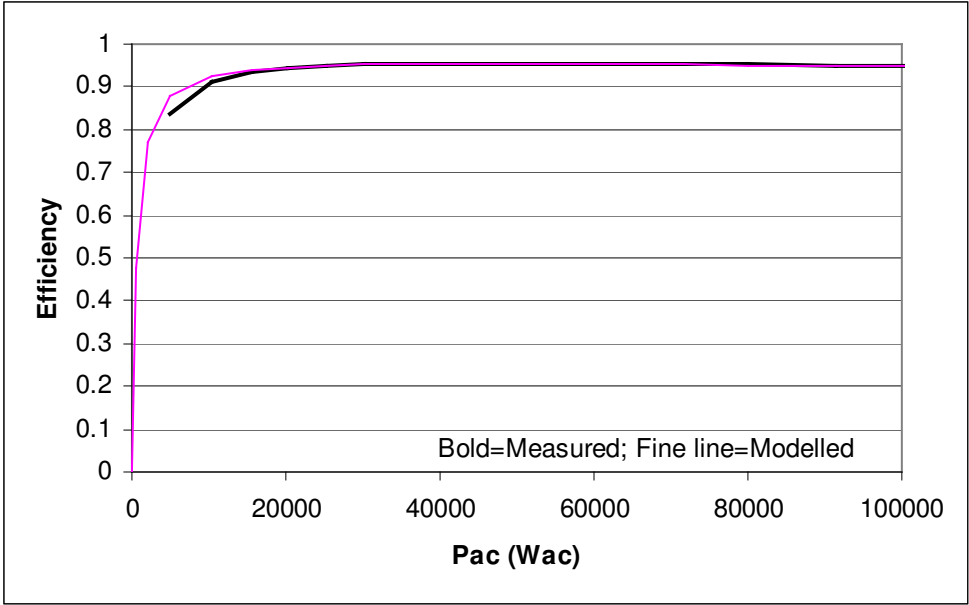


Figure 6.3 Efficiency of Omnion Series 3200 (100kW)

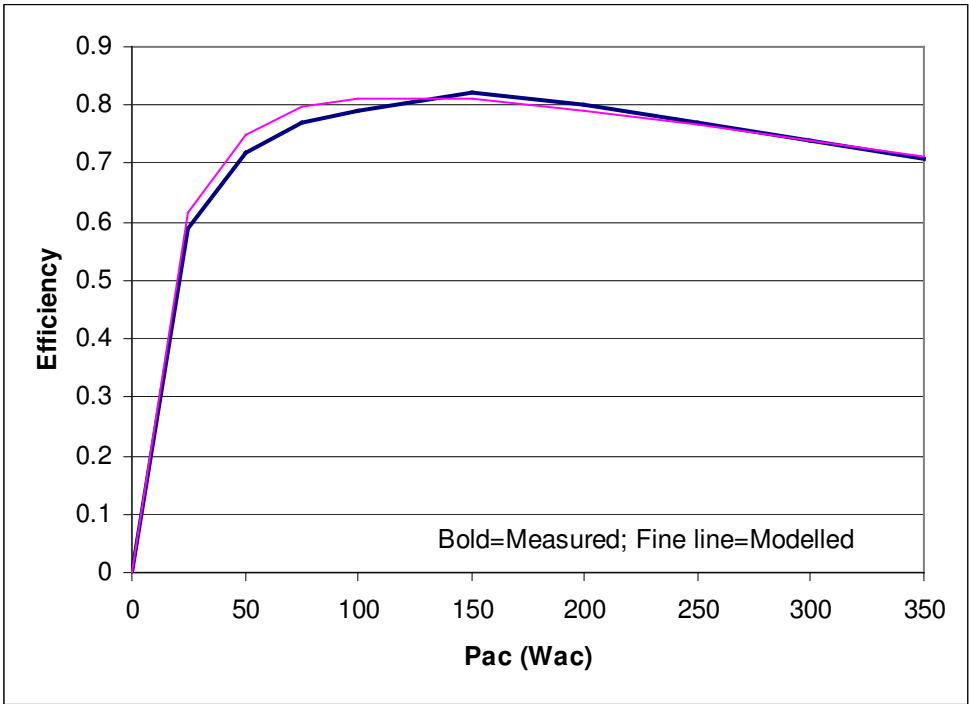


Figure 6.4 Efficiency of Rainbow 12V (300W)

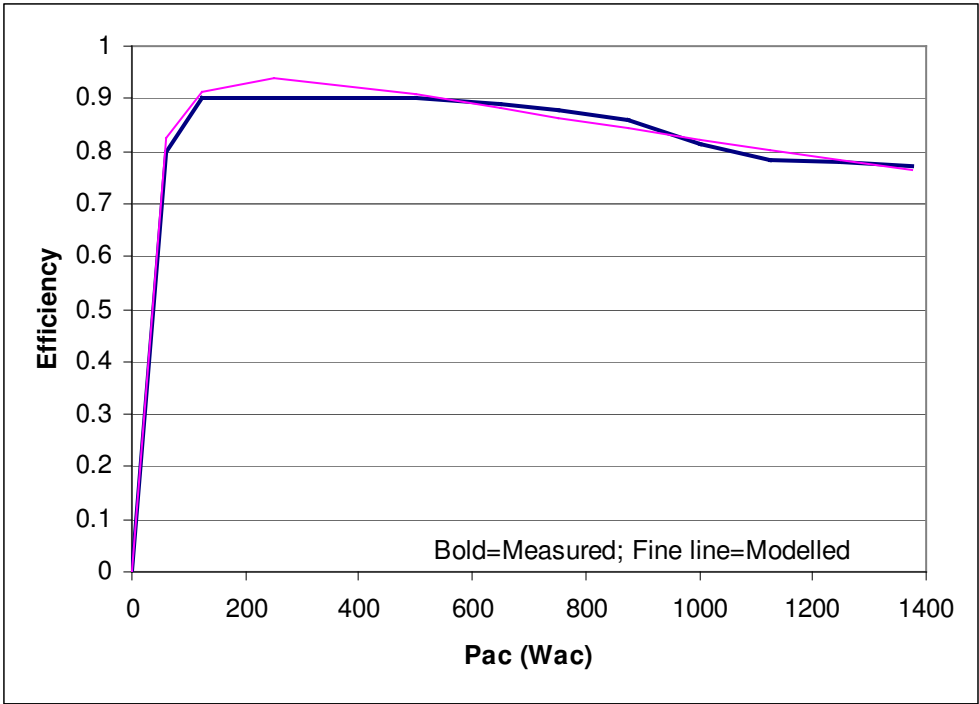


Figure 6.5 Efficiency of Selectronic SA21 (1200 W)

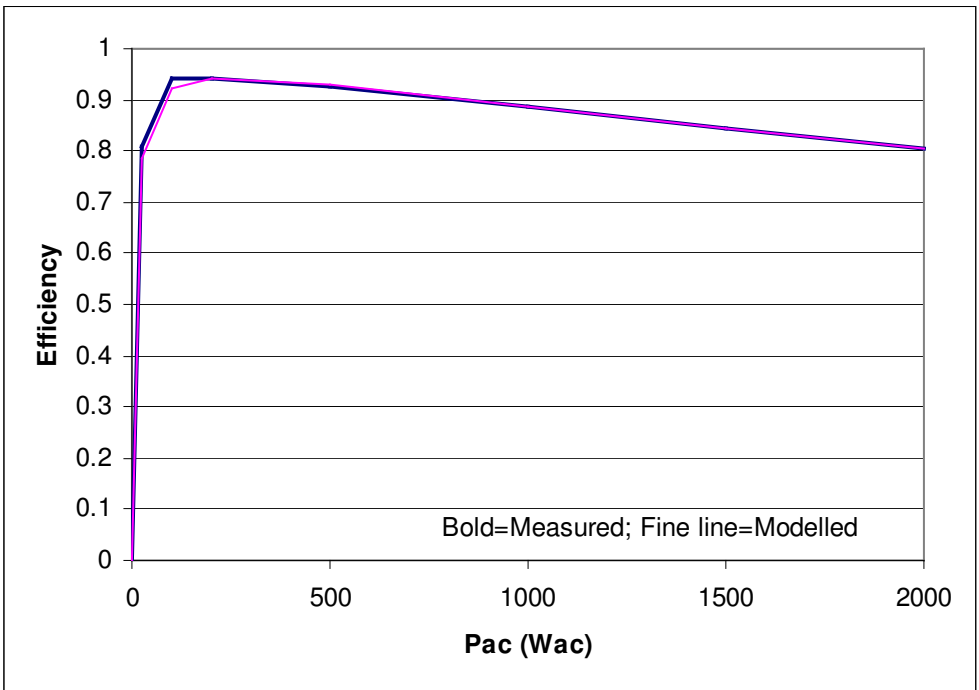


Figure 6.6 Efficiency of Trace DR1512 (1500 W)

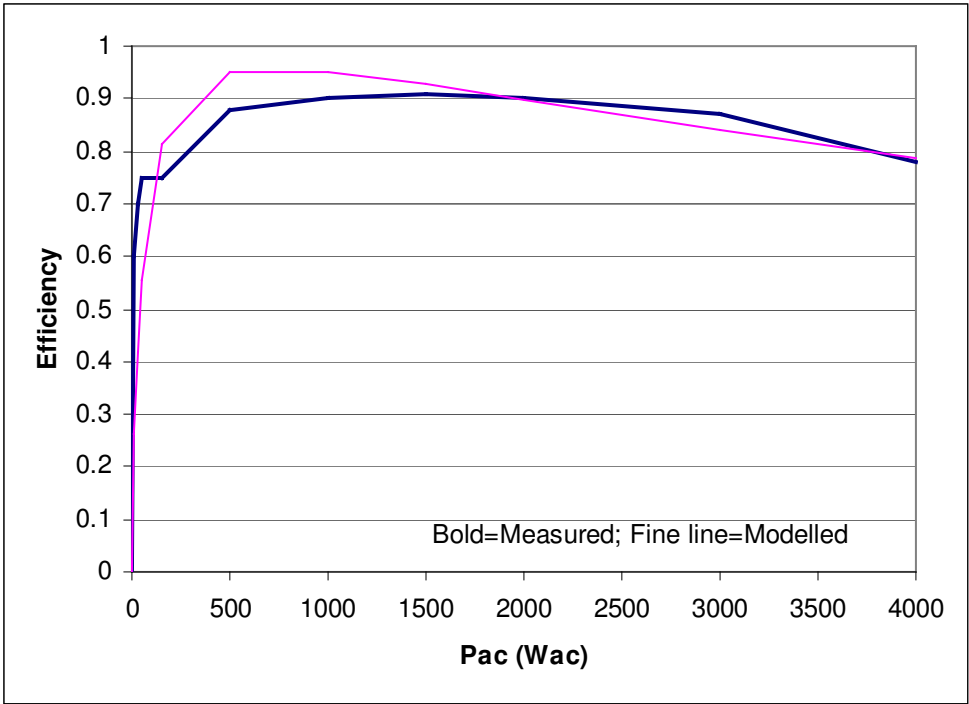


Figure 6.7 Efficiency of Vanner TSC24-4000D (4 kW)

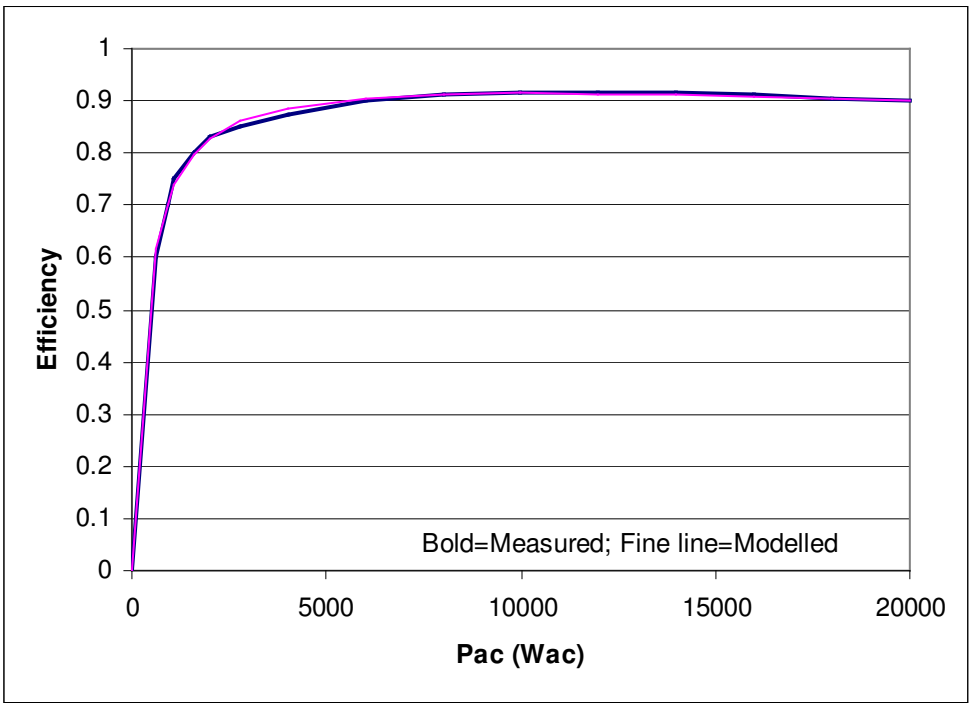


Figure 6.8 Efficiency of Solarmax 20 (20 kW)

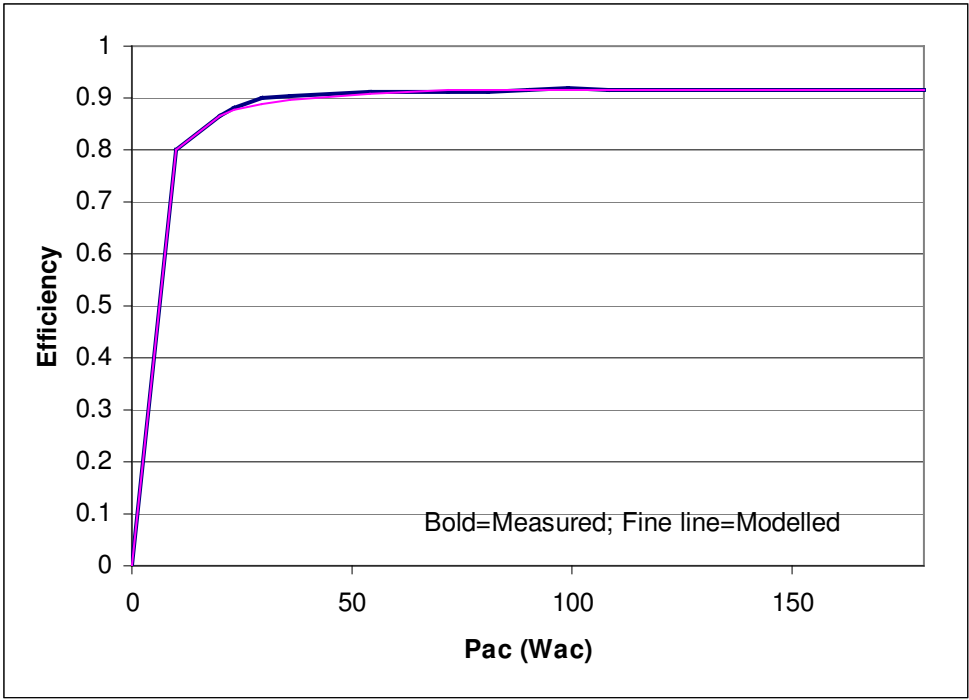


Figure 6.9 Efficiency of Edisun 200 (180 W)

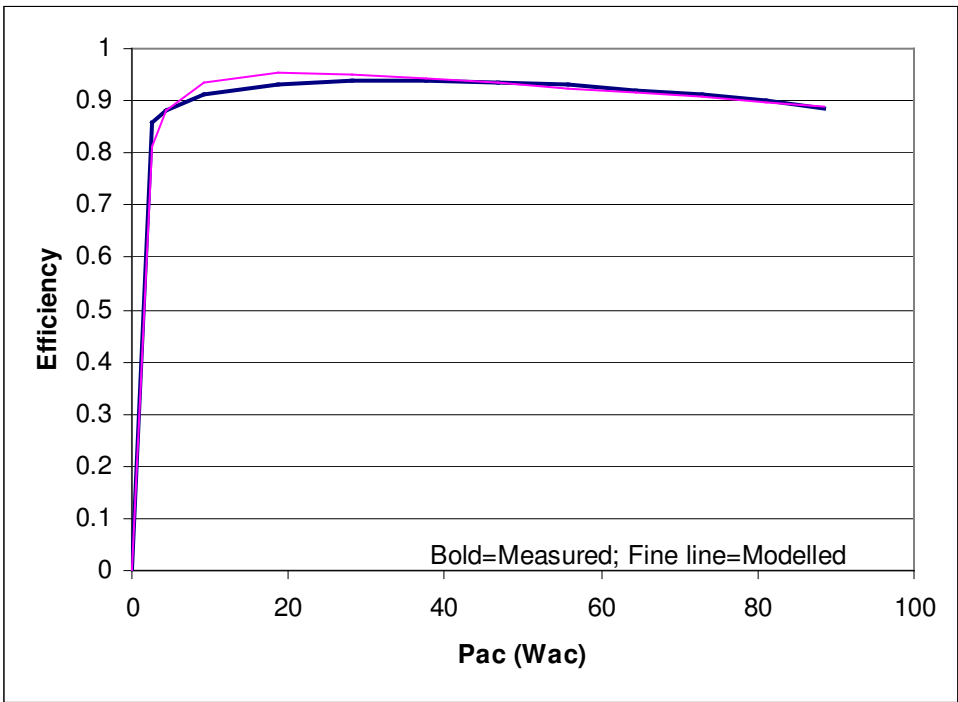


Figure 6.10 Efficiency of OK4 (100W)

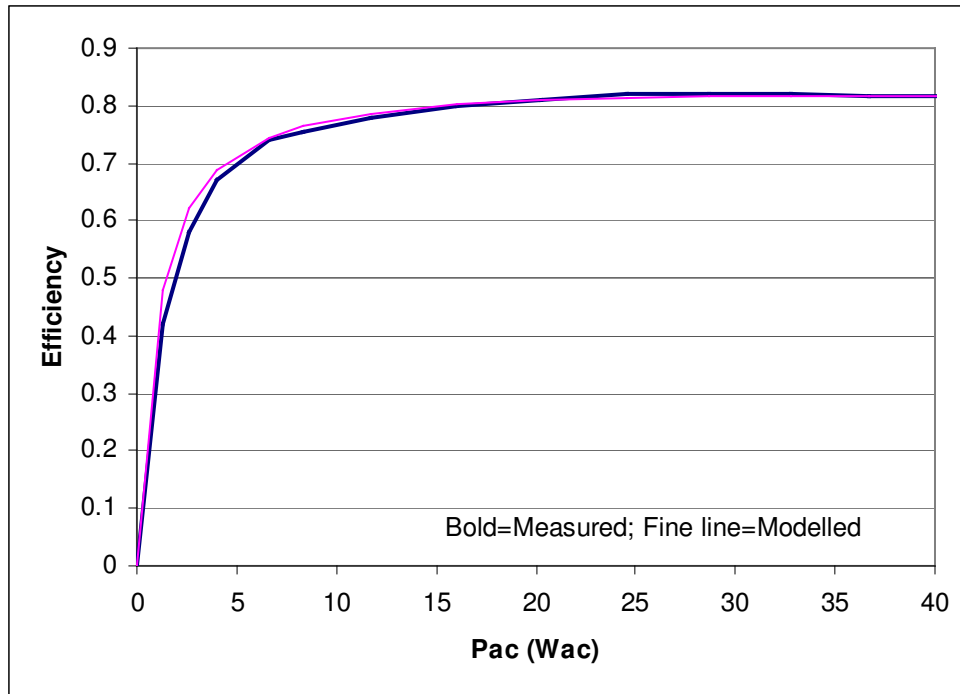


Figure 6.11 Efficiency of Weeber 50 (50W)

In general, the efficiency curve generated by the fit quadratic equation match the measured data very closely. Minor problems arise when the efficiency curve rises very sharply from 0, then plateaus through the middle range and finally drops significantly at high power. The high ohmic losses and sharp rise from zero result in a quadratic with high efficiency at the low end. If the efficiency curve is flat through the mid-range, then the quadratic will overestimate the efficiency at low power (see Figure 6.7). In addition, a quadratic equation can not mimic features in the efficiency curve such as local maximums and points of inflection (see Figures 6.1 and 6.5). Neither of these problems is especially significant.

The use of a single quadratic equation will probably not reproduce the complex efficiency curves of cascaded (“master-slave”) inverters. For these inverters, the use of multiple quadratic equations or higher order equations may be necessary. Peippo and Lund (1994) documents the use of multiple quadratic equations for cascaded inverters.

For the inverters in Figures 6.4, 6.5, 6.7 and 6.10, the least-squares fit coefficient for the linear loss term was less than one. This implies negative linear losses, or voltage gains rather than voltage drops: this is not physically realistic. This does not invalidate the approach, but merely suggests that the physical meaning of the coefficients should be interpreted loosely.

The existing approach does not accord temperature a role in the behaviour of the inverter. This is a reasonable assumption: it appears that most inverters will perform within specification over a range of operating temperatures from, say, 0°C to 40°C (see the Trace SW series specifications, for example). In some cases, the maximum power output of an inverter may fall with rising ambient air temperature.

## 6.2) Verification

Neither white box nor black box verification of the inverter model turned up any problems in the model implementation. For black box verification, the points used to describe the inverter efficiency curves of three of the inverters in Section 6.1 were used as parameters for the model. Then the coefficients for the fit quadratic equation were compared: in all three cases, they were identical for the Matlab<sup>®</sup> procedure and the Excel procedure. As a second part of this test, the inverter model was provided with a ramp input which ranged from 0 Watts to the nominal power of the inverter. The output was divided by the input and the resulting efficiency curve graphed. The curves matched the Excel curves. Finally, the Operation and Maintenance vector was examined to ensure that the “lifetimes used” variable was calculated correctly.

## 7) Genset

### 7.1) Validation

The genset model is intended to provide an estimate of the power output, fuel consumption, and wear caused by a certain level of demand under a given set of conditions, such as altitude and temperature.

When it is on, the genset has a power output that is assumed equal to the lesser of the AC demand and its maximum output, adjusted for temperature and altitude. The adjustment is performed according to the equation:

$$P_{adj} = P_{rated} \cdot \frac{p}{p_{rated}} \cdot \sqrt{\frac{T_{rated}}{T}}$$

where  $P_{adj}$  is the maximum power of the genset, adjusted for temperature and pressure,

$P_{rated}$  is the rated maximum output power of the genset,

$p$  is the atmospheric pressure,

$p_{rated}$  is the pressure at which the rated maximum power of the genset is measured,

$T$  is the temperature of the air entering the genset (in K),

and  $T_{rated}$  is the temperature at which the rated maximum power of the genset is measured (in K).

This equation for adjustment is standard and can be considered valid. For example, Heywood gives this correction factor in [Heywood, 1988, p. 55], although he indicates that the measured partial pressure of water vapour in the ambient air should be subtracted from the atmospheric pressure. Here the partial pressure of water vapour is not available, and the equation assumes that the air is perfectly dry. This should not lead to significant errors, since the partial pressure of water vapour should be quite low compared with the absolute air pressure. In the genset model,  $p_{rated}$  is assumed to be 98.2 kPa and  $T_{rated}$  is assumed to be 302.4 K; these are the standard conditions given by Heywood.

The atmospheric pressure,  $p$ , is estimated based on the altitude,  $z$ , according to the equation:

$$p = p_0 \cdot e^{\frac{-g \cdot z}{R \cdot T}}$$

where  $p_0$  is the atmospheric pressure at sea level (assumed to be 101.3 kPa),  
 $g$  is the acceleration due to gravity (assumed to be 9.8067 m/s<sup>2</sup>),  
 $R$  is the dry air gas constant (assumed to be 287.04 J kg<sup>-1</sup> K),  
 $z$  is the altitude, in m,  
and  $T$  is the temperature, in K.

This is a standard equation that is derived by assuming that air behaves as an ideal gas and integrating the hydrostatic equation for a column of air. For the purposes of the PV Toolbox it should be sufficiently accurate. For the genset model,  $p_0$  is assumed to be 101.3 kPa and  $T$  is assumed to be 21°C; these are reasonable assumptions.

The fuel consumption of the genset is, according to the model, linearly related to the power demand. In general, the fuel consumption of the genset will be non-zero at no load, but this is left for the user to specify. This approximation originally proposed by Reiniger et al. (1986), is widely considered valid for simulation of energy flows in hybrid systems (e.g., see Skarstein and Uhlen (1989), van Dijk (1996), and Manwell et al. (1996)).

In the current version of the model, the heat transferred from the genset to the environment is treated very simply. The useful work being extracted from the genset (i.e., the output power) is subtracted from the “power” contained in the fuel being consumed by the genset. That is, heating power is calculated by:

$$P_{heat} = \eta_{combust} \cdot V_{fuel} \cdot Q_{LHV} - P$$

where  $P_{heat}$  is the rate of heat transfer from the genset (e.g., in kW),  
 $\eta_{combust}$  is the combustion efficiency,  
 $V_{fuel}$  is the volume rate of fuel consumption (e.g., L/hour),  
 $Q_{LHV}$  is the lower heating value of the fuel on a volumetric basis (e.g., kWh/L),  
and  $P$  is the electrical power output of the genset (e.g., kW).

Fundamentally, this approach is sound—it is based on the principle of conservation of energy. The approach will be accurate to the extent that the fuel consumption is modelled accurately and the constants for combustion efficiency and heating value of the fuel are accurate. Errors in the modelling of the fuel consumption will lead to proportional errors in  $P_{heat}$ . The combustion efficiency is assumed to be 98% for diesel engines and 96% for gasoline engines; this should be relatively close to reality (see Heywood (1988), p. 82). The lower heating value of the fuel is a reasonable choice since the water in the exhaust will be in the gaseous phase. Although the density—and therefore the heat content—of the fuel will change with temperature, the fuel consumption rate is not adjusted on the basis of temperature so this does not cause a problem. For gasoline, an energy content of 44.0 MJ/kg and a density of 0.722 kg/L is assumed; for diesel fuel, these figures are 42.5 MJ/kg and 0.846 kg/L. These are reasonable assumptions according to published figures for these fuels.

While the approach is accurate, it will not be especially useful in the study of the utilisation of waste heat from the genset. For this, the heat output must be specified in terms of amount going to exhaust, amount going to coolant, amount radiated to environment, etc. It is recommended that the model be expanded to provide rudimentary information of this nature before it is used to study waste heat utilisation.

The lifetime, maintenance interval, and frequency of overhaul are handled very simply as well. The on-time of the genset is integrated; when this integral reaches the lifetime of the genset, as specified by the user, the genset needs replacement. Similarly, it is assumed that maintenance is required after every 500 h of operation. The frequency of overhauls for diesel gensets, on the other hand, is determined by the genset loading. When the genset is loaded between 50 and 100% of its nominal power, then it is assumed to deteriorate at a rate of one overhaul for every half lifetime. Below 50% rated power, the rate of deterioration rises linearly, such that at 0% of its nominal power, the rate of deterioration is equivalent to one overhaul every quarter lifetime. It is assumed that gasoline gensets will not be overhauled.

This approach seems plausible, but it is difficult to find solid support for it in the literature. Clearly low part load operation accelerates deterioration of the genset such that overhauls will be required more frequently. But is the rate as given? And does this part load operation have no effect on the ultimate lifetime of the genset or the interval at which it requires basic maintenance? A perusal of the literature does not validate the approach used, and it is recommended that the questions of lifetime, maintenance, and overhaul intervals be investigated more thoroughly.

An additional, though minor, concern with this approach is the use of the unadjusted nominal power for the denominator in the part load fraction. Should this be the nominal power, adjusted for temperature and altitude? Or, put another way, does altitude influence the interval between overhauls? If not, then the denominator should be the adjusted maximum power of the genset.

## **7.2) Verification**

Neither white box nor black box testing revealed any problems in the model. In the first black box test, the ambient temperature was set to 25°C and the altitude to 0 m. A ramp was used for power demand. For the nominally 10 kW genset, the ramp varied from –1 kW to 12 kW load. It was verified that the power output, fuel consumption, and heat output of the genset varied linearly between appropriate no load values (when demand was 0 or less) to appropriate full load values (when demand was around 10.4 kW or more). For the second black box test, the altitude was raised to 3000 m; it was confirmed that maximum output fell to roughly 70% of sea level values. For the third black box test, altitude was set to sea level and the temperature set to –5°C; it was confirmed that this raised maximum output roughly 5%. For the fourth black box test, altitude was set to sea level, the temperature to 25°C, the load to 10.4 kW, and the lifetime to 1500 hours; it was verified that after 1500 hours, exactly one life had been used and two overhauls and three maintenance visits had been required. For the fifth black box test, the load was set to 5.2 kW; it was verified that after 1500 hours, the situation was identical to that for the fourth black box test. In the sixth black box test, the load was set to 0 kW; it was verified that this resulted in four overhauls being required at 1500 hours.

## **8) Other components**

The tester developed the following components:

- Battery: A simple but comprehensive model that includes some information on aging and heat evolution.
- Rectifier: An AC to DC converter that is modelled in the same way as the inverter.
- Bulk/Absorb/Float Charge Controller: Although based on a controller originally developed by Sheriff and Turcotte, very significant changes have essentially resulted in a new component model. The changes were necessitated by simulation instabilities in the original model. A more flexible charging algorithm and equalisation charging were also added.
- Genset/PV Charge Controller: A Bulk/Absorb/Float charge controller for use in hybrid systems; this component is based on the charge controller model described above.
- On/Off Charge Controller: Control is achieved through interrupting the current completely.
- Genset Start: Applies a set of user-defined criteria to determine when the genset should start.
- Genset Stop: Applies a set of user-defined criteria to determine when the genset should stop.
- Loading Controller: Applies a set of user-defined criteria to determine how hard the genset should operate.
- Control Center: The interface between loads, generators, converters, storage, and controllers in a hybrid system.

Other than the battery, these components have not yet been validated; they are not covered in this document. It should be noted that the controllers and the control center are qualitatively different from the components examined in this document, and this suggests that a different validation and verification procedure may be appropriate.

The components studied in this document derive their behaviour directly from the physics underlying the devices. In the case of the controllers, the physics of the device are less important than the design and operation parameters decided upon, somewhat arbitrarily, by the architects of the device. For instance, an on/off charge controller could be implemented in an analog circuit, a digital circuit, a programmable logic controller, or even an electro-mechanical device, but the input-output characteristics could be the same for all these different implementations. Similarly, two identical analog circuits could have different input-output characteristics depending on the settings of potentiometers in the circuit.

The validation and the verification should therefore focus on comparing the specifications for various controllers with the output from the models. A representative selection of controllers should be used to draft a specification for the capabilities of the model. Then these capabilities should be tested by running the model. White box verification will be useful mainly for identifying pathological test cases where the model may fail.

## **9) System Models**

### **9.1) Background**

The component models validated/verified in this document, as well as component models developed by the tester and validated/verified elsewhere, have been integrated into system models that simulate the behaviour of PV hybrid systems of various configurations. During the course of this integration, it was found that component models that functioned flawlessly in isolation caused serious problems in system models. This necessitated many changes to certain components, particularly the charge controller and the battery. These changes generally did not alter the behaviour of the model, but simply made it more compatible with the components to which it is attached.

In more complex system models, feedback loops tie a component's output to its input. For example, battery voltage determines the PV array operating point which in turn determines the array output current which in turn influences the battery voltage. Furthermore, the controllers introduce significant non-linear behaviour to the system models. Simulink<sup>®</sup>, the tool that has been used to implement these models, is ideally suited to linear models that can be implemented as a set of simultaneous first-order differential equation. Feedback loops and non-linear components pose difficulties for Simulink<sup>®</sup>. These are manifested as 1) simulation halted with an error message when the set of equations can not be resolved, 2) simulation "freezing" at a point in time when instability in a variable forces the time-step to an almost infinitesimal duration, 3) the simulation running unacceptable slowly.

These problems were solved in various ways. Changes to the component models, sometimes informed by nothing more than trial and error, were necessary. The choice of solver and solution parameters proved important. The introduction of one-time step delays in certain variables, so as to break feedback loops, also improved stability. These various modifications, documented in the tester's laboratory notebooks, resulted in working system models.

## 9.2) Approach and Procedure

The testing of these system models did not follow the same approach as described for the component models. Whereas the goal of the validation and verification was to ensure accuracy, the testing of the system models was intended to ensure the compatibility of the components with each other. Thus the output of the system models was not compared with other simulations or monitored data, but rather inspected to see whether the results were reasonable. Generally, incompatibilities were easy to identify because they caused the simulation to halt or freeze. Also, verifying that battery voltage, power output, battery state-of-charge, current, etc. were in reasonable ranges confirmed that the system model was functioning correctly.

The simulation parameters used for all of the system model tests are as follows:

- Solver:
    - Start and stop times: See particular test
    - ODE45 (Dormand Price) variable time step solver
    - Max step size: 1; Initial step size: Auto
- Relative tolerance:  $1 \times 10^{-7}$ ; Absolute tolerance: Auto
- Refine output, factor: 1
  - Diagnostic options:
    - Consistency checking: Off

- Disable zero cross detection: Not Checked (i.e., zero cross detection enabled)
- Disable optimized block I/O storage: Not Checked
- Relax boolean type checking: Checked

The weather data for all system model tests was generated by Watgen for St. Hubert, Québec. The file is “sthubert.tmy”. The simulations were run on a 400 MHz Pentium® II with 132 MB of memory operating Windows NT® 4.0 Service Pack 6. Matlab® version 5.3.1 (R11.1) was used. During the simulations, other software were sometimes operating on the computer; the run-times of the simulations are simply meant to be indicative, therefore.

### 9.3) System Model Tests

#### 9.3.1) PV MPPT Array/Load

File: pvload1.mdl

Simulation Time: 0 to 8760 hours (1 year)

Run Time: 2 min 54 secs

Components & Parameters:

- Tilt:
  - Time zone: -5
  - Longitude: -73.5°
  - Latitude: 45°
  - PV azimuth: 0°
  - Slope: 45°
  - Path: c:\watgen\sthubert.tmy
  - Monthly albedo: 0.7, 0.7, 0.44, 0.2, 0.2, 0.2, 0.2, 0.2, 0.2, 0.2, 0.7
- PV at MPPT
  - Rated current: 5.9 A
  - Voc: 21.7 V
  - Rated voltage: 17 V
  - NOCT: 45°C
  - Change in Voc with temperature: -0.34%/°C
  - Irradiance coefficient: 0.085
  - MPPT efficiency: 95%
  - Cell efficiency: 12%
  - Maintenance rate: 5 years
  - Lifetime: 20 years
  - *Ta held at 25°C*

Notes: Successful test.

#### 9.3.2) PV Array/Load

File: pvload2.mdl

Simulation Time: 0 to 8760 hours (1 year)

Run Time: 3 min 15 secs

Components & Parameters:

- Tilt: see 9.3.1
- PV module
  - Rated current: 5.9 A
  - Voc: 21.7 V
  - Rated voltage: 17 V
  - Isc: 6.4 V
  - NOCT: 45°C
  - Change in Voc with temperature:  $-0.34\%/^{\circ}\text{C}$
  - Change in Isc with temperature: 0.04
  - Cell efficiency: 12%
  - Maintenance rate: 5 years
  - Lifetime: 20 years
  - *Ta held at 25°C*
- Load: 4.25 ohm resistor connected at all times and determining array voltage

Notes: Successful test.

### 9.3.3) PV MPPT Array/Battery/Load

File: pvldbat1.mdl

Simulation Time: 0 to 8760 hours (1 year)

Run Time: 13 min 8 secs

Components & Parameters:

- Tilt: see 9.3.1
- PV at MPPT: see 9.3.1
- Battery
  - Nominal Voltage: 12 V
  - Battery Capacity at 25°C,  $I=C/20$ : 200 Ah
  - Technology: Global Yuasa Tubular Flooded
  - Self Discharge in a Month: 5% at 25°C
  - Float Life: 10 years at 25°C
  - Linear cycle life estimation
  - Cycles: 1500 cycles at 50% DOD, 800 cycles at 80% DOD
  - Permissible water loss: 0.8 kg
  - Initial SOC: 30%
- Load: A 32 W load connected for 2 hours and then off for 6 hours.

Notes: Successful test.

### 9.3.4) PV Array/Battery/Load

File: pvldbat2.mdl

Simulation Time: 0 to 8760 hours (1 year)

Run Time: 14 min 53 secs

Components & Parameters:

- Tilt: see 9.3.1
- PV module: see 9.3.2
- Battery: see 9.3.3
- Load: A 5 Ohm resistor connected for 2 hours then off for 6 hours.

Notes: Successful test.

### 9.3.5) PV MPPT Array/Battery/Charge Controller/Loads

File: pvcc1.mdl

Simulation Time: 0 to 8760 hours (1 year)

Run Time: 25 min 11 secs

Components & Parameters:

- Tilt: see 9.3.1
- PV at MPPT: see 9.3.1
- Battery: see 9.3.3
- Charge controller:
  - Rated current: 6 Amps
  - Bulk Voltage: 14.5 V
  - Float Voltage: 13.5 V
  - End of Absorption current: 1 Amp
  - Absorption time: 3 hours
  - Equalisation voltage: 15.1 V
  - Equalisation duration: 1 hour
  - Interval between equalisation: 720 h
  - Equalisation trigger: Charge transferred:  $10^8$  Ah
  - Equalisation trigger: minimum voltage: 11.5 V
  - Equalisation trigger: minimum SOC: -10
  - Temperature compensation:  $-0.03$  V/°C
  - Setpoint floor: 13 V
  - MTTF: 10000 hours
- Loads:
  - Constant power load of 12 W connected for 2 hours and then off for 8 hours.
  - Resistance of 16 Ohms connected for 4 hours and then off for 12 hours.
  - A constant current load of 0.4 Amps connected for 5 hours then off for 5 hours.

Notes: Successful test.

### 9.3.6) PV Array/Battery/Charge Controller/Loads

File: pvcc2.mdl

Simulation Time: 0 to 8760 hours (1 year)

Run Time: 25 min 13 secs

Components & Parameters:

- Tilt: see 9.3.1
- PV module: see 9.3.2
- Battery: see 9.3.3
- Charge controller: see 9.3.5
- Loads: see 9.3.5

Notes: Successful test.

### 9.3.7) PV MPPT Array/Battery/On-Off Charge Controller/Loads

File: pvcc1.mdl

Simulation Time: 0 to 8760 hours (1 year)

Run Time: 16 min 15 secs

Components & Parameters:

- Tilt: see 9.3.1
- PV at MPPT: see 9.3.1
- Battery: see 9.3.3
- On Off CC:
  - Rated current: 6 Amps
  - Disconnect Voltage: 14.8 V
  - Float Voltage: 13.0 V
  - Maximum trickle charge current: 1 Amp
  - Equalisation disconnect voltage: 15.4 V
  - Interval between equalisation: 720 h
  - Equalisation trigger: Charge transferred:  $10^8$  Ah
  - Equalisation trigger: minimum voltage: 11.5 V
  - Equalisation trigger: minimum SOC: -10
  - Temperature compensation:  $-0.03$  V/°C
  - MTTF: 10000 hours
- Loads: see 9.3.5

Notes: Successful test. On several occasions, the voltage spiked above the setpoint when there was a large, instantaneous drop in the load. This did not cause instability, and may be realistic.

### 9.3.8) PV Array/Battery/On-Off Charge Controller/Loads

File: pvonoff2.mdl

Simulation Time: 0 to 8760 hours (1 year)

Run Time: 17 min 17 secs

Components & Parameters:

- Tilt: see 9.3.1
- PV module: see 9.3.2
- Battery: see 9.3.3

- Charge controller: see 9.3.7
- Loads: see 9.3.5

Notes: Successful test. On several occasions, the voltage spiked above the setpoint when there was a large, instantaneous drop in the load. This did not cause instability, and may be realistic.

### 9.3.9) PV MPPT Array/Battery/On-Off Charge Controller/Loads/Inverter

File: pvinv1.mdl

Simulation Time: 0 to 8760 hours (1 year)

Run Time: 21 min 8 secs to 8200 hours (estimated time to 8760 hours—22 min 34 secs)

Components & Parameters:

- Tilt: see 9.3.1
- PV at MPPT: see 9.3.1
- Battery: see 9.3.3
- Charge Controller: see 9.3.5
- Inverter:
  - No load consumption: 0.5 W
  - Nominal power: 120 W
  - Efficiency Curve: 76.6% at 5W, 87.1% at 10W, 93.6% at 20W, 95.8% at 50W, 93.6% at 80W, 90.7% at 100W, 87.8% at 120W.
  - MTTF: 100000 Hours
- Loads:
  - Constant power load of 8 W connected for 2 hours and then off for 8 hours.
  - Resistance of 16 Ohms connected for 4 hours and then off for 12 hours.
  - A constant current load of 0.35 Amps connected for 5 hours then off for 5 hours.
  - AC load on inverter of 100 Watts connected for 2 hours then off for 98 hours.

Notes: Test ran successfully until 8200.7 hours. At this point, low winter-time insolation had caused the state of charge to fall below -15% (negative state-of-charge being possible since the metric is given in terms of the C/20 capacity). When the 100 W inverter load came on, the discharge current could not be met by the inverter. The battery voltage dropped, and as a consequence, the current draw due to the constant power load rose. The test terminated with an error message when the discharge current reached 120 Amperes; the battery had been drawn down to 1 V. System behaviour under these conditions is outside the requirements of the simulation, and therefore the test can be considered a success. It does point out, however, the need for a low voltage disconnect.

### 9.3.10) Genset/Battery/Control Center/Loads/Inverter/Rectifier

File: hynopv.mdl

Simulation Time: 0 to 8760 hours (1 year)

Run Time: 11 min 55 secs

Components & Parameters:

- Battery: see 9.3.3
- Inverter: see 9.3.9
- Genset:
  - Fuel: Diesel
  - Nominal Power: 0.35 kW
  - Nominal Fuel Consumption: 0.15 L/kWh
  - No Load Consumption: 25% of full load
  - Lifetime: 50,000 h
  - Altitude: 100 m
  - $T_a$ : 25 °C
- Rectifier:
  - Minimum AC input: 0.5 W<sub>AC</sub>
  - Nominal power: 120 W<sub>AC</sub>
  - Efficiency Curve: 76.6% at 5W<sub>DC</sub>, 87.1% at 10W, 93.6% at 20W, 95.8% at 50W, 93.6% at 80W, 90.7% at 100W, 87.8% at 120W.
  - MTTF: 100000 Hours
- Control Center:
  - Genset/PV CC:
    - Bulk Voltage: 14.5 V
    - Float Voltage: 13.5 V
    - End of Absorption current: 1 Amp
    - Absorption time: 3 hours
    - Equalisation voltage: 15.1 V
    - Equalisation duration: 1 hour
    - Interval between equalisation: 720 h
    - Equalisation trigger: Charge transferred: 10<sup>8</sup> Ah
    - Equalisation trigger: minimum voltage: 11.5 V
    - Equalisation trigger: minimum SOC: -10
    - Temperature compensation: -0.03 V/°C
    - Setpoint floor: 13 V
    - MTTF: 10000 hours
  - Genset Controller:
    - Hour to Solar Hour
      - Time Zone: -5
      - Longitude: -73.5°
    - Genset Start:
      - First preferred start time: 25 (disabled)
      - Second preferred start time: 25 (disabled)
      - Absolute minimum temperature: 0°C
      - Max period genset stays off: 240 hours
      - High load turn on: 1 kW
      - Absolute minimum battery voltage: 12 V
      - Absolute minimum SOC: 0.5
      - Max equalize wait time: 50 hours

- Genset Stop:
  - Priority 1: Emergency shutdown when temperature reaches: 100°C
  - Priority 2a: Minimum run time: 1 h
  - Priority 2a: Minimum temperature: -100°C
  - Priority 2b: High load condition falls turns off genset: selected
  - Priority 2c: Minimum voltage: 14 V
  - Priority 2c: Minimum SOC: 0.6 (in terms of C/20 capacity)
  - Priority 2c: Wait until equalisation finished: selected
  - Priority 3: Minimum voltage: 16 V
  - Priority 3: Minimum SOC: 2 of C/20 (in terms of C/20 capacity)
  - Priority 3: Genset loading below: -1
  - Priority 3: Change in SOC: 2 (in terms of C/20 capacity)
  - Priority 3: Charge controller reaches: Float
- Loading Controller:
  - Operating Strategy: Specified Loading
  - Target Genset Loading Fraction: 1
  - Equalisation strategy: Ignore
  - Desired minimum genset loading fraction: 0
  - Rectifier size: 0.12 kW<sub>AC</sub>
  - Dump load maximum: 0 kW
- Loads:
  - DC power load of 10 W connected for 10 hours and then off for 10 hours.
  - Resistance of 16 Ohms connected for 4 hours and then off for 12 hours.
  - A constant current load of 0.35 Amps connected for 5 hours then off for 5 hours.
  - AC Power load of 10 Watts connected for 4 hours then off for 26 hours.

Notes: Successful test.

### 9.3.11) PV MPPT Array/Genset/Battery/Control Center/Loads/Inverter/Rectifier

File: hypv1.mdl

Simulation Time: 0 to 8760 hours (1 year)

Run Time: 37 min 55 secs

Components & Parameters:

- Battery: see 9.3.3
- Inverter: see 9.3.9
- Genset: see 9.3.10
- Rectifier: see 9.3.10
- Control Center:
  - CC Current Limit:
    - PV Current Limit: 6 Amps
  - Genset/PV CC: see 9.3.10
  - Genset Controller:
    - Hour to Solar Hour: see 9.3.10

- Genset Start:
  - First preferred start time: 20:00
  - Apply when: NeedEq is either high or low
  - Min SOC for 1<sup>st</sup> preferred start time: 0.6
  - Min battery voltage for 1<sup>st</sup> preferred start time: 12 V
  - Max equalize wait time for 1<sup>st</sup> preferred start time: 40 h
  - Min temperature for 1<sup>st</sup> preferred start time: -100°C
  - Second preferred start time: 25 (disabled)
  - Absolute minimum temperature: 0°C
  - Max period genset stays off: 240 hours
  - High load turn on: 0.1 kW
  - Absolute minimum battery voltage: 11.5 V
  - Absolute minimum SOC: 0.4
  - Max equalize wait time: 50 hours
- Genset Stop:
  - Priority 1: Emergency shutdown when temperature reaches: 100°C
  - Priority 2a: Minimum run time: 1 h
  - Priority 2a: Minimum temperature: -100°C
  - Priority 2b: High load condition falls turns off genset: selected
  - Priority 2c: Minimum voltage: 14 V
  - Priority 2c: Minimum SOC: 0.6 (in terms of C/20 capacity)
  - Priority 2c: Wait until equalisation finished: selected
  - Priority 3: Minimum voltage: 16 V
  - Priority 3: Minimum SOC: 2 of C/20 (in terms of C/20 capacity)
  - Priority 3: Genset loading below: -1
  - Priority 3: Change in SOC: 2 (in terms of C/20 capacity)
  - Priority 3: Renewables meet load: selected
  - Priority 3: Charge controller reaches: Absorb
- Loading Controller:
  - Operating Strategy: Specified Loading
  - Target Genset Loading Fraction: 1
  - Equalisation strategy: Ignore
  - Desired minimum genset loading fraction: 0.5
  - Rectifier size: 0.12 kW<sub>AC</sub>
  - Dump load maximum: 0 kW
- Loads:
  - DC power load of 30 W connected for 10 hours and then off for 10 hours.
  - Resistance of 8 Ohms connected for 4 hours and then off for 12 hours.
  - A constant current load of 1 Amp connected for 5 hours then off for 5 hours.
  - AC Power load of 100 Watts connected for 2 hours then off for 28 hours.

Notes: Successful test. Two minor concerns: at a number of places there was instantaneous voltage and current spike, e.g., at the end of absorb charging. The

simulation paused for several seconds numerous times when the combination of loads created a situation that was difficult to resolve.

### 9.3.12) PV Module/Genset/Battery/Control Center/Loads/Inverter/Rectifier

File: hypv2.mdl

Simulation Time: 0 to 8760 hours (1 year)

Run Time: 38 min 58 secs

Components & Parameters:

- Battery: see 9.3.3
- Inverter: see 9.3.9
- Genset: see 9.3.10
- Rectifier: see 9.3.10
- Control Center:
  - CC Current Limit: see 9.3.11
  - Genset/PV CC: see 9.3.10
  - Genset Controller: see 9.3.11
- Loads: see 9.3.11

Notes: Successful test. Two minor concerns: at a number of places there was instantaneous voltage and current spike, e.g., at the end of absorb charging. The simulation paused for several seconds numerous times when the combination of loads created a situation that was difficult to resolve.

## 10) Conclusions

Validation and verification of the component models revealed a number of weaknesses, particularly in the weather modelling routines. Similarly, testing of system models turned up instabilities that caused the Simulink® simulation to freeze or halt. These concerns have been addressed, however, and the following models can now be considered valid and functional: weather modelling, PV generators, thermal reservoir, fuel reservoir, inverter and genset.

## References

Anderson, A. J. "PV Translation Equations: A New Approach". *AIP Conference Proceedings*, pp. 604-612, January 1996.

Anderson, A. J. *PV Translation Equations: A New Approach. Final Report for Task 1.0 NREL Subcontract No. TAD-4-14166-01*. Taylorsville, NC, USA: Sunset Technology, 1998.

Atmospheric Environment Service. *Canadian Climate Normals Volume I: Solar Radiation 1951-1980*. Ottawa, Canada: Environment Canada, 1982.

Bacha, John D. "Energy Resources, Conversion, and Utilisation: Liquid Petroleum Fuels" in Perry, Robert H., Don W. Green, and James O. Maloney, eds. *Perry's Chemical Engineers' Handbook, 7<sup>th</sup> Edition*. New York, New York: McGraw-Hill, 1997.

Brinkworth, B. J. "Autocorrelation and Stochastic Modelling of Insolation Sequences". *Solar Energy* Vol. 19 (1977) pp. 343-347.

DieselNet Technology Guide. "What is Diesel Fuel". [www.DieselNet.com](http://www.DieselNet.com), 2001.

Duffie, J. A. and W. A. Beckman. *Solar Engineering of Thermal Processes*. New York, N.Y.: Wiley-Interscience, 1991.

Erbs, Daryl G., Sanford A. Klein, William A. Beckman. "Estimation of Degree-Days and Ambient Temperature Bin Data from Monthly-Average Temperatures". *ASHRAE Journal*, June 1983, pp. 60-65.

Graham, V. A., K. G. T. Hollands, and T. E. Unny. "A Time Series Model for Kt with Application to Global Synthetic Weather Generation". *Solar Energy* Vol. 40, No. 2 (1988) pp. 83-92.

Graham, V. A., and K. G. T. Hollands. "A Method to Generate Synthetic Hourly Solar Radiation Globally". *Solar Energy* Vol. 44, No. 6 (1990) pp. 333-341.

Haeblerlin, H., F. Kaeser, Ch. Liebi, and Ch. Beutler. "Results of Recent Performance and Reliability Tests of the Most Popular Inverters for Grid Connected PV Systems in Switzerland." *13<sup>th</sup> European Photovoltaic Solar Energy Conference, 23-27 October, 1995, Nice, France*, Vol. I, pp. 585-590.

Haeblerlin, Ch. Liebi, and Ch. Beutler. "Inverters for Grid Connected PV Systems: Test Results of Some New Inverters and Latest Reliability of the Most Popular Inverters in Switzerland." *14<sup>th</sup> European Photovoltaic Solar Energy Conference, 30 June- 4 July, 1997, Barcelona, Spain*, Vol. II, pp. 2184-2187.

Heywood, John B. *Internal Combustion Engine Fundamentals*. New York, USA: McGraw-Hill Book Company, 1988.

IPL Information Processing Ltd. "An Introduction to Software Testing". Bath, United Kingdom: Information Processing Ltd., 1996.

Jantsch, Martin, Heribert Schmidt, and Jürgen Schmid. "Results of Concerted Action on Power Conditioning and Control". *11<sup>th</sup> European Photovoltaic Solar Energy Conference, 12-16 October, 1992, Montreux, Switzerland*, pp. 1589-1593.

Lorenzo, E. and L. Narvarte. "On the Usefulness of Stand-Alone PV Sizing Methods." *Progress in Photovoltaics: Research and Applications* Vol. 8 (2000) pp. 391-409.

Manwell, J. F., A. Rogers, G. Hayman, C. T. Avelar, J. G. McGowan. *Hybrid 2—A Hybrid System Simulation Model: Theory Summary*. Massachusetts, USA: Renewable Energy Research Laboratory, Department of Mechanical Engineering, University of Massachusetts, 1996.

McKay, D.C. and R.J. Morris. *Solar Radiation Data Analyses for Canada 1967-1976*. Ottawa, Canada: Environment Canada, 1985.

Mora-López, L. L. and M. Sidrach-de-Cardona. "Multiplicative ARMA Models to Generate Hourly Series of Global Irradiation". *Solar Energy* Vol 63, No. 5 (1998), pp. 283-291.

Oldenkamp, H., I. J. de Jong, C.W.A. Baltus, S.A.M. Verhoeven. "Advanced High Frequency Switching Technology of OK4 AC Module Inverters Break the 1 US\$/Watt Price Barrier." *14<sup>th</sup> European Photovoltaic Solar Energy Conference, 30 June- 4 July, 1997, Barcelona, Spain*, Vol. II, pp. 2218-2221.

Peippo, K. and P.D. Lund. "Optimal Sizing of Solar Array and Inverter in Grid-Connected Photovoltaic Systems". *Solar Energy Materials and Solar Cells* Vol 32 (1994), pp. 95-114.

Reiniger, K., T. Schott, and A. Zeidler. "Optimisation of hybrid stand-alone systems." *Proceedings of the European Wind Energy Conference, 7-9 October, 1986, Rome, Italy*.

Remund, Jan, and Stefan Kunz. *Meteonorm*. Bern, Switzerland: Meteotest, 1997.

Schmidt, Heribert. "From the Solar Cell to the Solar Generator". In *Photovoltaic Systems*, edited by Georg Hille, Werner Roth, and Heribert Schmidt. Freiburg, Germany: Fraunhofer Institute for Solar Energy Systems, 1995.

Skarstein, Øyvind and Kjetil Uhlen. "Design Considerations with Respect to Long-Term Diesel Saving in Wind/Diesel Plants". *Wind Engineering* Vol. 13 No. 2 (1989) pp. 72-87.

Thevenard, Didier. *Energy Rating of PV Modules (August 1999 Report)*. Waterloo, Ontario, Canada: Numerical Logics Inc., 1999.

van Dijk, Vincent A. P. *Hybrid Photovoltaic Solar Energy Systems*. Doctoral Thesis, University of Utrecht. The Netherlands, 1996.

Vartiainen, E. "A New Approach to Estimating the Diffuse Irradiance on Inclined Surfaces". *Renewable Energy*, Vol 20 (2000) pp.45-64.

Wilk, Heinrich and Gerd Schauer. "Operational Behaviour of Small Power Conditioners for Grid Interactive PV Systems (AC Modules)" *14<sup>th</sup> European Photovoltaic Solar Energy Conference, 30 June- 4 July, 1997, Barcelona, Spain*, Vol. II, pp. 2225-2228.